

Robust, randomized preconditioning for kernel ridge regression*

Mateo Díaz[†] Ethan N. Epperly[‡] Zachary Frangella[§] Joel A. Tropp[‡]
 Robert J. Webber[‡]

Abstract

This paper investigates preconditioning techniques for solving kernel ridge regression (KRR) problems with a medium to large number of data points ($10^4 \leq N \leq 10^7$), and it introduces two new methods with state-of-the-art performance. The first method, RPCHOLESKY preconditioning, accurately solves the full-data KRR problem in $\mathcal{O}(N^2)$ arithmetic operations, assuming sufficiently rapid polynomial decay of the kernel matrix eigenvalues. The second method, KRILL preconditioning, offers an accurate solution to a restricted version of the KRR problem involving $k \ll N$ selected data centers at a cost of $\mathcal{O}((N + k^2)k \log k)$ operations. The proposed methods efficiently solve a broad range of KRR problems, making them ideal for practical applications.

1 Motivation

Kernel ridge regression (KRR) is a machine learning method for learning an unknown function $y = f(\mathbf{x})$ from a set of input–output pairs

$$(\mathbf{x}^{(1)}, y_1), (\mathbf{x}^{(2)}, y_2), \dots, (\mathbf{x}^{(N)}, y_N) \in \mathcal{X} \times \mathbb{R},$$

where the inputs take values in an arbitrary set \mathcal{X} . KRR is based on a positive-definite kernel $K : \mathcal{X} \times \mathcal{X} \rightarrow \mathbb{R}$ that captures the “similarity” between a pair of inputs. KRR produces a nonlinear prediction function $\hat{f} : \mathcal{X} \rightarrow \mathbb{R}$ of the form

$$\hat{f}(\mathbf{x}) = \sum_{i=1}^N \beta_i K(\mathbf{x}^{(i)}, \mathbf{x})$$

that models the input–output relationship. KRR is widely used in data science and scientific computing, for example, in predicting the chemical properties of molecules [18, 54]. Section 2 provides more details about KRR.

In practice, KRR is often limited to small- or medium-sized data sets ($N \leq 10^4$) because the computation time can grow rapidly with the number of data points. KRR involves linear algebra computations with the $N \times N$ kernel matrix \mathbf{A} with entries $a_{ij} = K(\mathbf{x}^{(i)}, \mathbf{x}^{(j)})$. To obtain the prediction function \hat{f} , we must solve an $N \times N$ positive-definite linear system to high accuracy, which requires $\mathcal{O}(N^3)$ arithmetic operations using the standard direct method based on Cholesky

*ENE acknowledges support from DOE CSGF DE-SC0021110. MD, JAT, and RJW acknowledge support from ONR BRC N00014-18-1-2363, from NSF FRG 1952777, and from the Caltech Carver Mead New Adventures Fund. ZF acknowledges support from NSF IIS-1943131, the ONR Young Investigator Program, and the Alfred P. Sloan Foundation.

[†]Department of Applied Mathematics & Statistics, Johns Hopkins University, Baltimore, MD (mateodd@jhu.edu).

[‡]Computing & Mathematical Sciences, California Institute of Technology, Pasadena, CA (eepperly@caltech.edu, jtropp@caltech.edu, rwebber@caltech.edu).

[§]Management Science & Engineering, Stanford University, Stanford, CA (zfran@stanford.edu).

decomposition. Because of this poor computational scaling, survey articles on machine learning for scientific audiences (such as [51]) suggest using KRR for small data sets and neural networks for larger data sets. Reliably scaling KRR to larger data sets with $N \geq 10^4$ remains an open research challenge.

To improve the scalability of KRR, two main approaches have been developed. The first approach aims to solve the full-data KRR problem accurately in $\mathcal{O}(N^2)$ operations using preconditioned conjugate gradient (CG) [5, 16]. The second approach *restricts* the KRR problem to a small number of $k \ll N$ centers chosen from the data points [48] and aims to solve the restricted problem in $\mathcal{O}(kN)$ operations using preconditioned CG [44].

However, due to the ill-conditioned nature of many KRR problems, CG-based approaches can only succeed when there is a high-quality preconditioner. Consequently, much of the research on solving KRR problems over the past decade has focused on proposing preconditioners [16, 22, 23, 44, 45, 47], empirically testing preconditioners [8, 16, 47], and theoretically analyzing preconditioners [5, 22, 23, 44, 45]. Despite this extensive body of work, a user of KRR might struggle to identify the best preconditioner, since many ideas have been proposed and there has not been a recent comparison of the available approaches.

The primary purpose of a preconditioner is to minimize the number of CG iterations required to solve a linear system to a desired level of accuracy. For KRR, each CG iteration can be computationally expensive as it involves either one multiplication with the $N \times N$ kernel matrix (for full-data KRR) or two multiplications with the $N \times k$ kernel submatrix (for restricted KRR). Additionally, the kernel matrix or submatrix may not fit in working memory, in which case kernel matrix entries must be accessed from storage or regenerated from data at each CG iteration, which adds to the computational cost. This paper seeks to reduce the expense of KRR by identifying preconditioners that are both efficient to construct and capable of controlling the number of CG iterations required for convergence.

To be useful in practice, a preconditioner must work *reliably* for a range of KRR instances, and it must be *robust* against adverse conditions (such as poorly conditioned kernel matrices). Additionally, the preconditioner should not require any delicate parameter tuning. Such a robust and no-hassle preconditioner is vital for general-purpose scientific software that can handle a variety of KRR problems framed by different users. Additionally, such a preconditioner is critical for cross-validation, as it enables searching for the best kernel model while having confidence that the preconditioner can handle the resulting linear systems efficiently. Unfortunately, as this paper shows, many existing KRR preconditioners are prone to failure when applied to specific KRR problems, limiting their range of applicability.

To meet the need for higher-quality preconditioners, this paper harnesses randomized matrix approximation schemes [12, 15] that have not been previously applied in the context of KRR but are valuable for achieving robustness. We use these approximations to devise two new *randomized* preconditioners that allow us to solve more KRR problems in fewer iterations than the techniques in current use [16, 22, 23, 44, 45]. The RPCHOLESKY preconditioner (Algorithm 1) can be applied to the full-data KRR problem, while the KRILL preconditioner (Algorithm 2) can be applied to the restricted KRR problem involving $k \ll N$ data centers. Both preconditioners are cheap to implement, are effective for a wide range of KRR problems, and are supported by strong theoretical guarantees.

The RPCHOLESKY preconditioner is designed to solve linear systems involving the full-data $N \times N$ kernel matrix. The preconditioning algorithm constructs a nearly optimal low-rank approximation of the kernel matrix [12], and the preconditioner employs a shift of this low-rank approximation. Under favorable eigenvalue decay conditions, RPCHOLESKY preconditioning brings the number of CG iterations down to acceptable levels (10^0 – 10^2). Yet it is important to recognize that any

preconditioner based on low-rank approximation, including RPCHOLESKY, requires that the rank of the kernel approximation is at least as high as the number of large eigenvalues in the kernel matrix. Thankfully, many problems in scientific machine learning *do* exhibit sufficient eigenvalue decay for this approach to be successful: see Section 4.1 for a case study drawn from quantum chemistry.

The KRILL preconditioner is designed to solve restricted KRR problems (Section 2.2), which are linear systems involving an $N \times k$ submatrix of the full $N \times N$ kernel matrix. KRILL constructs a preconditioner by performing dimensionality reduction on the $N \times k$ kernel submatrix using a sparse random sign embedding [15]. KRILL is consistently successful in numerical tests, as it reduces the number of CG iterations to acceptable levels (10^0 – 10^2) *regardless* of the kernel matrix eigenvalue decay. Due to this reliability and robustness, just as krill are the foundation for the marine ecosystem, KRILL can serve as the foundation for large-scale KRR applications in the future

1.1 Plan for paper

The rest of this paper is organized as follows. Section 2 presents the RPCHOLESKY and KRILL preconditioning strategies; Section 3 compares RPCHOLESKY and KRILL to other preconditioners; Section 4 applies the RPCHOLESKY and KRILL preconditioners to benchmark problems in computational chemistry and physics; Section 5 contains proofs of the theoretical results; and Section 6 offers conclusions.

1.2 Notation

For simplicity, we focus on the real setting, although our work extends to complex-valued kernels without significant modification. The transpose and Moore–Penrose pseudoinverse of \mathbf{A} are denoted \mathbf{A}^* and \mathbf{A}^\dagger . Double bars $\|\cdot\|$ indicate the Euclidean norm of a vector or the spectral norm of a matrix. The matrix condition number is $\kappa(\mathbf{A}) := \|\mathbf{A}\| \|\mathbf{A}^{-1}\|$. For a positive-definite matrix \mathbf{M} , the \mathbf{M} -weighted inner product norm is denoted $\|\mathbf{z}\|_{\mathbf{M}} := (\mathbf{z}^* \mathbf{M} \mathbf{z})^{1/2}$. The function $\lambda_i(\mathbf{M})$ outputs the i th largest eigenvalue of \mathbf{M} . The ℓ_1 norm of the vector \mathbf{x} is denoted by $\|\mathbf{x}\|_{\ell_1} = \sum_i |x_i|$. The symbol $|S|$ denotes the cardinality of a set S .

2 Algorithms and best practices

For the KRR user’s convenience, this early section highlights our recommended approaches for solving KRR problems. Specifically, Section 2.1 introduces the RPCHOLESKY preconditioner for solving the full-data KRR problem, while Section 2.2 introduces the KRILL preconditioner for solving the restricted KRR problem.

2.1 Full-data kernel ridge regression

Recall that we are given N input–output data pairs $(\mathbf{x}^{(1)}, y_1), (\mathbf{x}^{(2)}, y_2), \dots, (\mathbf{x}^{(N)}, y_N)$ in $\mathcal{X} \times \mathbb{R}$ for training. Assume that $K : \mathcal{X} \times \mathcal{X} \rightarrow \mathbb{R}$ is a positive-definite kernel function, and define the $N \times N$ positive-semidefinite kernel matrix \mathbf{A} with numerical entries $a_{ij} = K(\mathbf{x}^{(i)}, \mathbf{x}^{(j)})$.

In full-data kernel ridge regression (KRR), we build a prediction function of the form

$$\hat{f}(\mathbf{x}; \boldsymbol{\beta}) = \sum_{i=1}^N \beta_i K(\mathbf{x}^{(i)}, \mathbf{x}).$$

Algorithm 1 RPCHOLESKY preconditioning

Input: Positive semidefinite matrix $\mathbf{A} \in \mathbb{R}^{N \times N}$, right-hand-side vector $\mathbf{y} \in \mathbb{R}^N$, regularization coefficient μ , approximation rank r , and tolerance ε .

Output: Approximate solution β_\star to $(\mathbf{A} + \mu\mathbf{I})\beta = \mathbf{y}$.

- 1: $\mathbf{F} \leftarrow \text{RPCHOLESKY}(\mathbf{A}, r, \min(100, r/10))$. ▷ See Algorithm 4.
- 2: $(\mathbf{U}, \Sigma, \sim) \leftarrow \text{ECONOMYSIZESVD}(\mathbf{F})$. ▷ $\hat{\mathbf{A}} = \mathbf{U}\Sigma^2\mathbf{U}^*$.
- 3: Define primitives for preconditioned conjugate gradient:

$$\text{Product} : \beta \mapsto \mathbf{A}\beta + \mu\beta.$$

$$\text{Preconditioner} : \beta \mapsto \mathbf{U} \left[(\Sigma^2 + \mu\mathbf{I})^{-1} - \mu^{-1}\mathbf{I} \right] \mathbf{U}^*\beta + \mu^{-1}\beta.$$

- 4: $\beta_\star \leftarrow \text{PCG}(\text{Product}, \mathbf{y}, \varepsilon, \text{Preconditioner})$. ▷ See Algorithm 3.
-

The coefficients $\beta \in \mathbb{R}^N$ for the function are chosen to minimize the regularized least-squares loss function

$$L(\beta) = \|\mathbf{y} - \mathbf{A}\beta\|^2 + \mu\beta^* \mathbf{A}\beta.$$

Here, $\mu > 0$ is a regularization parameter. Theoretical literature [9] suggests setting the regularization to $\mu = \mathcal{O}(N^p)$ for a value $p \in (0, 2/3)$ depending on the kernel matrix eigenvalue decay and the smoothness of f . In practice, μ is typically chosen via cross-validation or a grid search.

Minimizing $L(\beta)$ is a quadratic optimization problem whose solution β satisfies

$$(\mathbf{A} + \mu\mathbf{I})\beta = \mathbf{y}. \tag{2.1}$$

The linear system can be solved in $\mathcal{O}(N^3)$ time using a Cholesky decomposition of $\mathbf{A} + \mu\mathbf{I}$ and two triangular solves. However, if there is a medium or large number of data points ($N \geq 10^4$), we instead recommend solving (2.1) at a reduced cost using conjugate gradient with RPCHOLESKY preconditioning, described below. We will prove that RPCHOLESKY solves the full-data KRR problem in $\mathcal{O}(N^2)$ time, provided the kernel matrix eigenvalues decay at a sufficiently fast polynomial rate (Theorem 2.2).

2.1.1 RPCholesky preconditioning

To build a preconditioner for the full-data KRR equations (2.1), we begin with a low-rank approximation $\hat{\mathbf{A}}$ of the kernel matrix \mathbf{A} . Then, we define the preconditioner

$$\mathbf{P} = \hat{\mathbf{A}} + \mu\mathbf{I}. \tag{2.2}$$

There are many ways to obtain a low-rank approximation for this purpose, and we adopt the recently popular RPCHOLESKY algorithm (Algorithm 4, analyzed in [12]).

The RPCHOLESKY algorithm is a variant of partial Cholesky decomposition that chooses random pivots at each step according to an evolving probability distribution. For an input parameter $r \in \mathbb{N}$, the algorithm returns a rank- r approximation in factorized form:

$$\hat{\mathbf{A}} = \mathbf{F}\mathbf{F}^* \quad \text{where } \mathbf{F} \in \mathbb{R}^{N \times r}.$$

The matrix $\hat{\mathbf{A}}$ is random because it depends on the choice of random pivots. On average, $\hat{\mathbf{A}}$ is comparable to the best rank- r approximation of \mathbf{A} , as established in [12, Thm. 3.1]. The algorithm

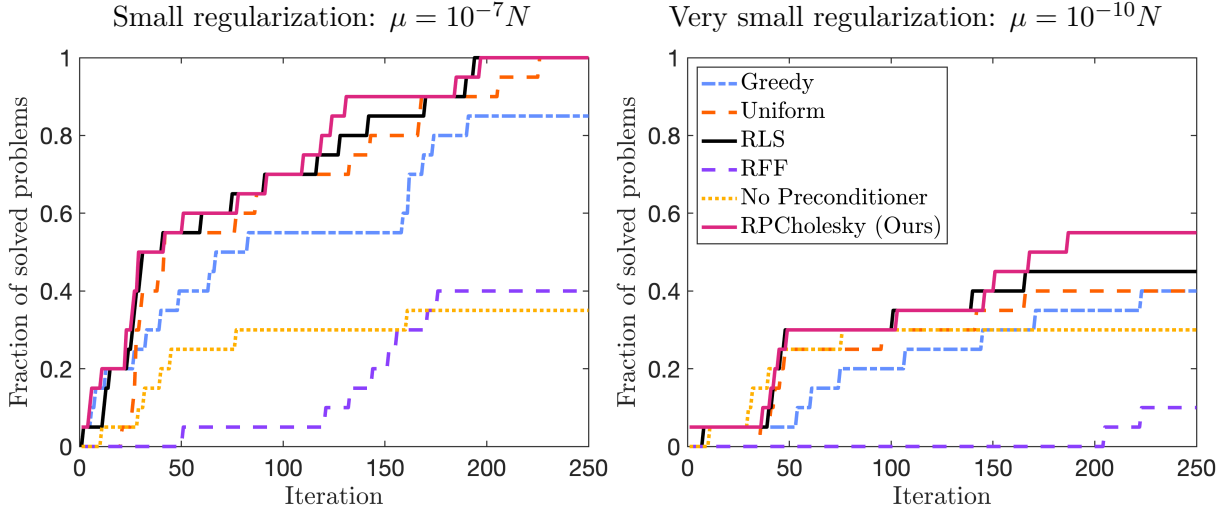


Figure 1: Fraction of solved problems versus number of CG iterations for the 20 KRR problem instances in Table 1.

accesses only $(r + 1)N$ entries of the kernel matrix; it uses $\mathcal{O}(rN)$ storage; and it expends $\mathcal{O}(r^2N)$ arithmetic operations.

We propose to select the approximation rank $r = \mathcal{O}(\sqrt{N})$, which ensures that we can obtain an eigenvalue decomposition of the preconditioner \mathbf{P} in $\mathcal{O}(N^2)$ operations. We then apply preconditioned CG (Algorithm 3, described in [24, §10.3]) to solve the KRR problem. Provided that $r = \mathcal{O}(\sqrt{N})$ suffices to obtain a good preconditioner, CG terminates in a constant number of iterations and the total operation count for RPCHOLESKY preconditioning is $\mathcal{O}(N^2)$. The pseudocode for RPCHOLESKY preconditioning is given in Algorithm 1.

2.1.2 Empirical performance

Next we test the empirical performance of RPCHOLESKY and four other preconditioners on the 20 regression and classification problems described in Table 1 of Appendix A. For each problem, we first randomly subsample $N = 1.5 \times 10^4$ data points. We standardize the features (subtract the mean, divide by the standard deviation) and measure similarity using the squared exponential kernel

$$K(\mathbf{x}, \mathbf{y}) = \exp\left(-\frac{1}{2\sigma^2}\|\mathbf{x} - \mathbf{y}\|^2\right) \quad \text{with bandwidth } \sigma = 3. \quad (2.3)$$

We then formulate each KRR problem (2.1) with a small regularization parameter $\mu/N = 10^{-7}$ (left panel) or a very small regularization parameter $\mu/N = 10^{-10}$ (right panel) and choose the rank r of the preconditioner to be $r = 1000$. This choice of parameters is typical for full-data KRR problems [5, 22], and the same parameters are applied uniformly over the 20 regression and classification problems without any additional tuning. Note the smaller value of μ makes many of these problems highly ill-conditioned. We run 250 CG iterations and declare each KRR instance to be “solved” as soon as the relative residual $\|(\mathbf{A} + \mu\mathbf{I})\boldsymbol{\beta} - \mathbf{y}\|/\|\boldsymbol{\beta}\|$ falls below an error tolerance of $\varepsilon = 10^{-3}$. This choice of ε is justified by the fact that the test error plateaus after reaching this tolerance for all of the problems we considered.

Figure 1 charts the fraction of solved problems when using RPCHOLESKY and four other preconditioners based on low-rank approximation. Two alternative pivoting schemes for partial Cholesky decomposition are greedy pivot selection [23, 53] and uniformly random pivot selection

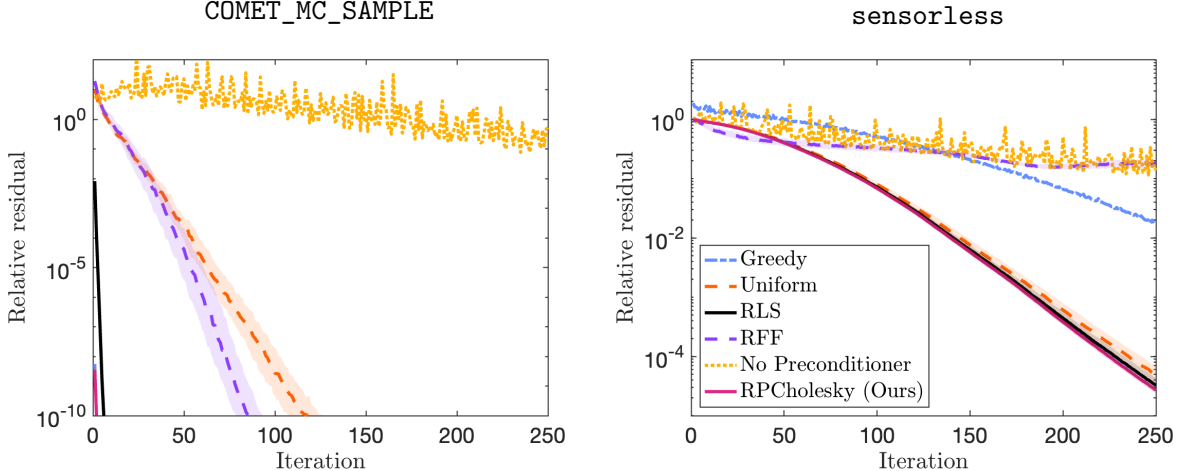


Figure 2: Relative residual versus number of CG iterations for the problem with the fastest (COMET_MC_SAMPLE, left) and slowest (sensorless, right) CG convergence when $\mu/N = 10^{-7}$. Note the different vertical axis scales.

[16, 22]. Two additional methods for randomized low-rank approximation are ridge leverage score sampling (RLS, [1, 36, 45]) and random Fourier features (RFF, [5, 16]). For details of these methods, see Section 3.1.

RPCHOLESKY is the top-performing method in Figure 1, both when the regularization is small (left) and when the regularization is very small (right). The closest competitor method is RLS, yet RPCHOLESKY consistently performs as well or better than RLS. For example, when $\mu/N = 10^{-7}$, RPCholesky and RLS lead to nearly the same number of CG iterations ($\pm 20\%$ differences) on 14 of the 20 test problems. On the remaining 6 problems, RPCHOLESKY converges $1.2\times$ – $2.4\times$ more quickly than RLS. As another advantage, RPCHOLESKY is simpler to implement and faster to run than RLS, as it eliminates the cost of approximating the ridge leverage scores (see Section 3.1).

We might worry that RPCHOLESKY changes behavior depending on the random seed, but empirically the algorithm produces consistent results with just $\pm 5\%$ random variation in the number of CG iterations. To illustrate this point, Figure 2 shows the distribution of the relative residual error $\|(\mathbf{A} + \mu\mathbf{I})\boldsymbol{\beta} - \mathbf{y}\|/\|\boldsymbol{\beta}\|$ for the two problems with the fastest (COMET_MC_SAMPLE) and the slowest (sensorless) CG convergence. The lines indicate the median error and the shaded regions indicate the 20%–80% error quantiles, which are computed over 100 random runs. The 20%–80% quantiles are hardly distinguishable from the median lines, and they are even tighter for RPCHOLESKY than the other stochastic methods (uniform, RLS, and RFF).

The importance of eigenvalue decay is evident from Figure 2. In the problem with rapid eigenvalue decay (COMET_MC_SAMPLE, left), RPCHOLESKY converges to the accuracy threshold $\varepsilon = 10^{-3}$ in just a single iteration. In the problem with slow eigenvalue decay (sensorless, right), RPCHOLESKY converges $200\times$ more slowly. All the methods based on low-rank approximation struggle to control the condition number for the sensorless problem, given that the eigenvalues of the kernel matrix decay slowly over 6 orders of magnitude. The dependence on eigenvalue decay is the main limitation of any preconditioner based on low-rank approximation. Nonetheless, even for this difficult problem, RPCHOLESKY and the other preconditioners significantly improve on unpreconditioned CG.

2.1.3 Theoretical guarantees

The sole requirement for RPCHOLESKY’s success is an eigenvalue decay condition which ensures the accuracy of the low-rank approximation $\hat{\mathbf{A}} \approx \mathbf{A}$. To explain this condition in detail, we introduce a quantitative measure of the eigenvalue decay called the μ -tail rank of the matrix \mathbf{A} :

Definition 2.1 (Tail rank). The μ -tail rank of a psd matrix $\mathbf{A} \in \mathbb{R}^{N \times N}$ is

$$\text{rank}_\mu(\mathbf{A}) := \min \left\{ r \geq 0 : \sum_{i>r} \lambda_i(\mathbf{A}) \leq \mu \right\}.$$

For example, in KRR problems with the squared exponential kernel (2.3), the μ -tail rank is $\mathcal{O}(\log(1/\mu)^d)$ where d is the intrinsic dimensionality of the data [2].

Next, we state our main performance guarantee for RPCHOLESKY preconditioning; the proof appears in Section 5.1.

Theorem 2.2 (RPCHOLESKY preconditioning). *Fix a failure probability $\delta \in (0, 1)$ and an error tolerance $\varepsilon \in (0, 1)$. Let \mathbf{A} be any positive-semidefinite matrix. Construct a random approximation $\hat{\mathbf{A}}$ using RPCHOLESKY with block size $B = 1$ and approximation rank*

$$r \geq \text{rank}_\mu(\mathbf{A}) (1 + \log(\text{tr } \mathbf{A}/\mu)). \quad (2.4)$$

With probability at least $1 - \delta$ over the randomness in $\hat{\mathbf{A}}$, the RPCHOLESKY preconditioner $\mathbf{P} = \hat{\mathbf{A}} + \mu \mathbf{I}$ controls the condition number at a level

$$\kappa(\mathbf{P}^{-1/2}(\mathbf{A} + \mu \mathbf{I})\mathbf{P}^{-1/2}) \leq 3/\delta. \quad (2.5)$$

Conditional on the event (2.5), when we apply preconditioned CG to the KRR linear system $(\mathbf{A} + \mu \mathbf{I})\boldsymbol{\beta} = \mathbf{y}$, we obtain an approximate solution $\boldsymbol{\beta}^{(t)}$ for which

$$\|\boldsymbol{\beta}^{(t)} - \boldsymbol{\beta}\|_{\mathbf{A} + \mu \mathbf{I}} \leq \varepsilon \cdot \|\boldsymbol{\beta}\|_{\mathbf{A} + \mu \mathbf{I}} \quad (2.6)$$

at any iteration $t \geq \delta^{-1/2} \log(2/\varepsilon)$, where $\boldsymbol{\beta}$ is the actual solution.

Theorem 2.2 ensures that RPCHOLESKY-preconditioned CG can solve any full-data KRR problem to fixed error tolerance ε with failure probability δ , provided that the eigenvalue condition (2.4) is satisfied. This eigenvalue condition ensures that the approximation rank r is large enough to reliably capture the large eigenvalues of the kernel matrix. The factor $\log(\text{tr } \mathbf{A}/\mu)$ is modest in size, being at most $\log(2^{53}) = 36.7$ in double-precision arithmetic. Thus, the expression (2.4) is mainly determined by the $\text{rank}_\mu(\mathbf{A})$ factor, which counts the number of “large” eigenvalues with the rest of the eigenvalues adding up to size μ or smaller.

If $\text{rank}_\mu(\mathbf{A})$ is $\mathcal{O}(\sqrt{N})$ and we apply RPCHOLESKY preconditioning with $r = \mathcal{O}(\sqrt{N})$ columns, Theorem 2.2 guarantees that we can solve any full-data KRR problem in $\mathcal{O}(N^2)$ operations. Uniform and greedy Nyström preconditioning admit no similar guarantee (see Section 3.1). Theorem 2.2 also provides insight into the case where the μ -tail rank is larger than $\mathcal{O}(\sqrt{N})$. In this case, we may need to use a larger approximation rank r , and the construction cost for the preconditioner would exceed $\mathcal{O}(N^2)$ operations.

Figure 3 evaluates RPCHOLESKY’s capacity to control the conditioning of the 20 example problems when $\mu/N = 10^{-7}$. Before RPCHOLESKY preconditioning, the condition numbers range from 10^4 – 10^7 . RPCHOLESKY typically reduces the condition number to 10^1 – 10^3 and sometimes even to 10^0 . However, RPCHOLESKY cannot fully control the conditioning for the most difficult problems, as no rank- r Nyström preconditioner can reduce the condition number beyond $(\lambda_{r+1}(\mathbf{A}) +$

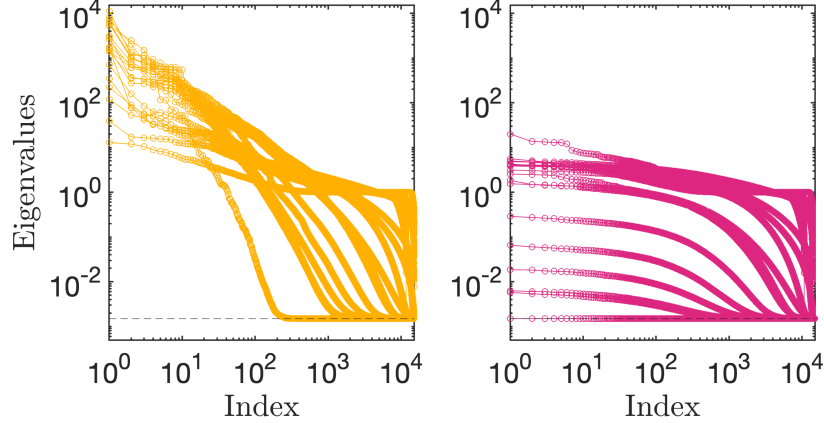


Figure 3: Eigenvalue decay for the 20 KRR problems in Table 1. Left panel shows eigenvalues of the matrix $\mathbf{A} + \mu\mathbf{I}$ before RPCHOLESKY preconditioning. Right panel shows eigenvalues of the matrix $\mu\mathbf{P}^{-1/2}(\mathbf{A} + \mu\mathbf{I})\mathbf{P}^{-1/2}$ after RPCHOLESKY preconditioning with $r = 1000$. Dashed line indicates the regularization parameter $\mu = 10^{-7}N$.

$\mu)/(\lambda_N(\mathbf{A}) + \mu)$. To further reduce the condition number, it would be necessary to significantly raise the approximation rank.

In practice, the parameter r should be tuned to balance the cost of forming the preconditioner and the cost of the CG iterations. As a simple default, we recommend setting $r = 10\sqrt{N}$. This default is $1.2\times$ larger than the approximation rank used in Figure 3 and is large enough to ensure that all 20 test problems are solved in fewer than 200 iterations when $\mu/N = 10^{-7}$. See Section 4.1 for more exploration of the parameter r with a scientific data set.

2.2 Restricted kernel ridge regression

If the number of data points is so large that we cannot apply full-data KRR, we pursue an alternative approach that we call “restricted KRR”, which was proposed in [48]. In restricted KRR, we build a prediction function

$$\hat{f}(\mathbf{x}; \hat{\boldsymbol{\beta}}) = \sum_{i=1}^k \hat{\beta}_i K(\mathbf{x}^{(s_i)}, \mathbf{x}),$$

using a subset $\mathbf{x}^{(s_1)}, \mathbf{x}^{(s_2)}, \dots, \mathbf{x}^{(s_k)}$ of input points, which are called “centers”. There are many strategies for selecting the centers, such as uniform sampling, ridge leverage score sampling, and RPCHOLESKY. One must balance the computational cost of the center selection procedure against the quality of the centers. For all experiments in this paper, we use the computationally trivial approach of sampling centers uniformly at random; however, the development of fast procedures for identifying high-quality centers is an interesting topic for future work.

In restricted KRR, the coefficients $\hat{\boldsymbol{\beta}}$ are chosen to minimize the loss function

$$L(\hat{\boldsymbol{\beta}}) = \|\mathbf{y} - \mathbf{A}(:, \mathbf{S})\hat{\boldsymbol{\beta}}\|^2 + \mu\hat{\boldsymbol{\beta}}^* \mathbf{A}(\mathbf{S}, \mathbf{S})\hat{\boldsymbol{\beta}},$$

where $\mathbf{A}(:, \mathbf{S})$ denotes the submatrix of \mathbf{A} with column indices in $\mathbf{S} = \{s_1, \dots, s_k\}$ and $\mathbf{A}(\mathbf{S}, \mathbf{S})$ denotes the submatrix with row and column indices both in \mathbf{S} . Minimizing this quadratic loss function leads to a coefficient vector $\hat{\boldsymbol{\beta}}$ that satisfies

$$[\mathbf{A}(\mathbf{S}, :)\mathbf{A}(:, \mathbf{S}) + \mu\mathbf{A}(\mathbf{S}, \mathbf{S})] \hat{\boldsymbol{\beta}} = \mathbf{A}(\mathbf{S}, :)\mathbf{y}. \quad (2.7)$$

Algorithm 2 KRILL preconditioning

Input: Positive semidefinite matrix $\mathbf{A} \in \mathbb{R}^{N \times N}$, right-hand-side vector $\mathbf{y} \in \mathbb{R}^N$, regularization coefficient μ , centers \mathbf{S} , and tolerance ε .

Output: Approximate solution $\hat{\beta}_*$ to $(\mathbf{A}(\mathbf{S}, :)\mathbf{A}(:, \mathbf{S}) + \mu \mathbf{A}(\mathbf{S}, \mathbf{S}))\hat{\beta} = \mathbf{A}(\mathbf{S}, :)\mathbf{y}$.

1: $\mathbf{H} \leftarrow \mu \mathbf{A}(\mathbf{S}, \mathbf{S})$

2: $\mathbf{H} \leftarrow \mathbf{H} + N\varepsilon_{\text{mach}} \text{tr}(\mathbf{A}(\mathbf{S}, \mathbf{S})) \cdot \mathbf{I}$.

$\triangleright \varepsilon_{\text{mach}} \approx 2 \times 10^{-16}$ in double precision.

3: $k \leftarrow |\mathbf{S}|$.

4: $\Phi \leftarrow \text{SPARSESIGNEMBEDDING}(d = 2k, N, \zeta = \min\{8, 2k\})$.

\triangleright See Algorithm 5.

5: $\mathbf{B} \leftarrow \Phi \mathbf{A}(:, \mathbf{S})$.

6: $\mathbf{P} \leftarrow \mathbf{B}^* \mathbf{B} + \mathbf{H}$.

7: $\mathbf{C} \leftarrow \text{CHOLESKY}(\mathbf{P} + \varepsilon_{\text{mach}} \text{tr}(\mathbf{P}) \cdot \mathbf{I})$.

8: Define primitives for preconditioned conjugate gradient:

$$\text{Product} : \hat{\beta} \mapsto \mathbf{A}(:, \mathbf{S})(\mathbf{A}(\mathbf{S}, :)\hat{\beta}) + \mathbf{H}\hat{\beta}.$$

$$\text{Preconditioner} : \hat{\beta} \mapsto \mathbf{C}^{-1}(\mathbf{C}^{-*}\hat{\beta}).$$

9: $\hat{\beta}_* \leftarrow \text{PCG}(\text{Product}, \mathbf{A}(\mathbf{S}, :)\mathbf{y}, \varepsilon, \text{Preconditioner})$.

\triangleright See Algorithm 3.

Equation (2.7) is a $k \times k$ linear system that is smaller than the system eq. (2.1) for the full-data KRR problem. This system can become highly ill-conditioned. To mitigate this issue, we add a small multiple of the machine precision $\varepsilon_{\text{mach}}$ to the diagonal entries of the regularizer $\mu \mathbf{A}(\mathbf{S}, \mathbf{S})$.

Solving (2.7) by direct methods is expensive because of the $\mathcal{O}(k^2 N)$ cost of forming the Gram matrix $\mathbf{G} = \mathbf{A}(\mathbf{S}, :)\mathbf{A}(:, \mathbf{S})$. When the number of centers is moderately large ($k \geq 10^3$), we recommend a cheaper approach for solving (2.7) using conjugate gradient with the KRILL preconditioner, described below. We will prove that KRILL preconditioning solves *every* restricted KRR problem in $\mathcal{O}((N + k^2)k \log k)$ arithmetic operations (Theorem 2.3).

2.2.1 KRILL preconditioning

The KRILL preconditioner is based on a randomized approximation of the Gram matrix $\mathbf{G} = \mathbf{A}(\mathbf{S}, :)\mathbf{A}(:, \mathbf{S})$. To form this approximation, first generate a sparse random sign embedding [29, §9.2]:

$$\Phi = \frac{1}{\sqrt{\zeta}} \begin{bmatrix} \phi_1 & \cdots & \phi_N \end{bmatrix} \in \mathbb{R}^{d \times N},$$

where ϕ_1, \dots, ϕ_N are sparse columns that possess uniform ± 1 values in ζ uniformly randomly chosen positions. Then, form the matrix $\mathbf{B} = \Phi \mathbf{A}(:, \mathbf{S})$ and compute the outer product matrix $\hat{\mathbf{G}} = \mathbf{B}^* \mathbf{B}$. Last, add a small multiple of $\mathbf{A}(\mathbf{S}, \mathbf{S})$ to $\hat{\mathbf{G}}$ to construct the KRILL preconditioner:

$$\mathbf{P} = \mathbf{B}^* \mathbf{B} + \mu \mathbf{A}(\mathbf{S}, \mathbf{S}) = (\Phi \mathbf{A}(:, \mathbf{S}))^* (\Phi \mathbf{A}(:, \mathbf{S})) + \mu \mathbf{A}(\mathbf{S}, \mathbf{S}). \quad (2.8)$$

The pseudocode for KRILL preconditioning is provided in Algorithm 2.

KRILL preconditioning is efficient because evaluating the approximate Gram matrix $\hat{\mathbf{G}}$ requires fewer operations than evaluating the exact Gram matrix \mathbf{G} . The precise number of operations depends on the sparsity ζ and the embedding dimension d . In our theoretical analysis, we assume $\zeta = \mathcal{O}(\log k)$ and $d = \mathcal{O}(k \log k)$, and we can form $\hat{\mathbf{G}}$ in $\mathcal{O}((N + k^2)k \log k)$ operations. In practice, we still observe fast CG convergence when we use a smaller, sparser embedding with $\zeta = \min\{8, 2k\}$ and $d = 2k$ [50, p. A2440]. Consequently, after including the cost of the CG iterations, the total operating cost of KRILL preconditioning is $\mathcal{O}((N + k^2)k \log k)$ in theory and $\mathcal{O}((N + k^2)k)$ in practice.

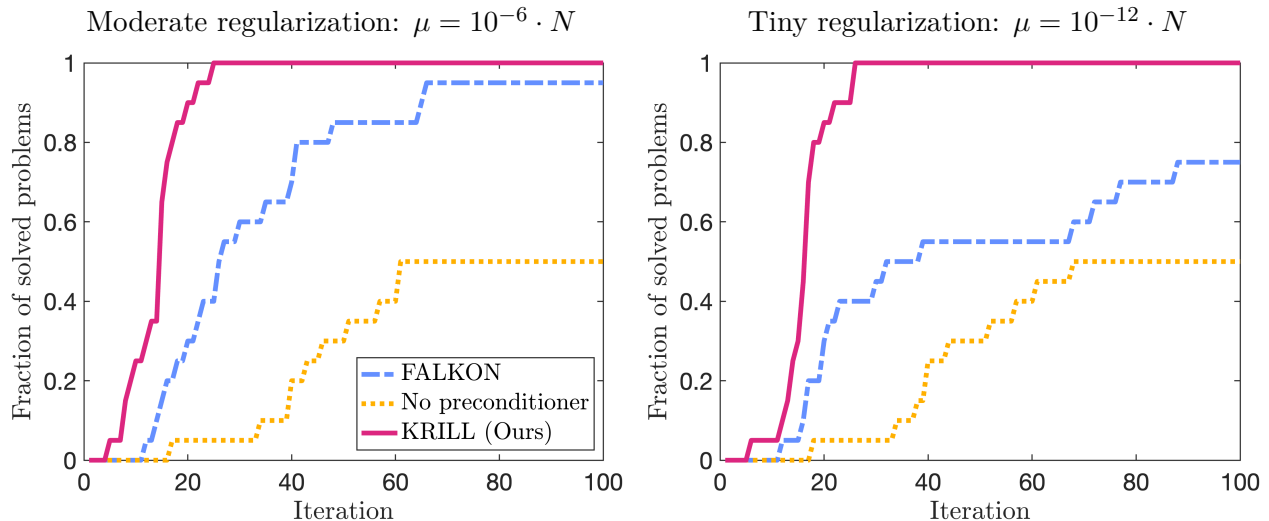


Figure 4: Fraction of solved problems versus number of CG iterations for the 20 kernel problems in Table 1.

2.2.2 Empirical performance

Figure 4 evaluates the performance of KRILL across the 20 regression and classification problems described in Table 1. For each problem, we subsample $N = 4 \times 10^4$ data points and select $k = 1000$ centers uniformly at random. We then standardize the features and apply KRR using the squared exponential kernel (2.3) with the bandwidth $\sigma = 3$. The regularization is either set to a moderate value $\mu/N = 10^{-6}$ or a tiny value $\mu/N = 10^{-12}$. We run 100 CG iterations and declare a problem to be “solved” if the relative residual

$$\frac{\|[\mathbf{A}(\mathbf{S}, \cdot)\mathbf{A}(\cdot, \mathbf{S}) + \mu\mathbf{A}(\mathbf{S}, \mathbf{S})]\hat{\boldsymbol{\beta}} - \mathbf{A}(\mathbf{S}, \cdot)\mathbf{y}\|}{\|\mathbf{A}(\mathbf{S}, \cdot)\mathbf{y}\|} \quad (2.9)$$

falls below a tolerance of $\varepsilon = 10^{-4}$. For comparison, Figure 4 also evaluates the performance of the current state-of-the-art solver FALKON, which approximates the Gram matrix \mathbf{G} via Monte Carlo sampling. For essential details of FALKON, see Section 3.2.

Examining Figure 4, we find that KRILL solves all of the classification and regression problems in 30 iterations, both when the regularization is moderate (left) and when the regularization is tiny (right). In contrast, FALKON struggles with the tiny regularization (right panel), and it solves just 9 problems after 30 CG iterations.

KRILL is a randomized algorithm, so it might change behavior depending on the random seed. Yet empirically, KRILL produces consistent results up to $\pm 10\%$ random variation in the number of CG iterations. Figure 5 shows the median and the 20%–80% quantiles of the relative residual eq. (2.9) for the problems with the fastest (*yolanda*, left) and slowest (*creditcard*, right) CG convergence. The quantiles are calculated using 100 random subsamples \mathbf{S} and subsequent CG solves. In these problems, the 20%–80% quantiles are highly concentrated around the median.

2.2.3 Theoretical guarantees

With the proper parameter choices, KRILL is guaranteed to solve any restricted KRR problem with any positive-semidefinite kernel matrix $\mathbf{A} \in \mathbb{R}^{N \times N}$ and any regularization parameter $\mu > 0$.

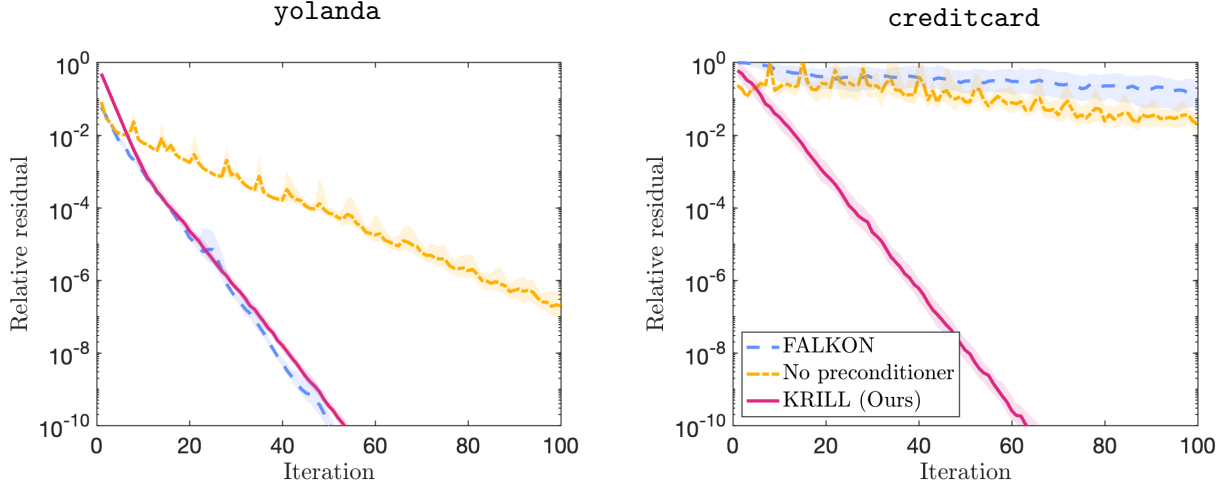


Figure 5: Relative residual versus number of CG iterations for the problems with the fastest (*yolanda*, left) and slowest (*creditcard*, right) CG convergence when $\mu/N = 10^{-6}$. Thick lines show the median error and shaded regions show the 20%–80% error quantiles over 100 random trials.

Unlike RPCholesky preconditioning, KRILL does not require any eigenvalue decay. Here, we state our main theoretical guarantee, which is proved in Section 5.2.

Theorem 2.3 (KRILL performance guarantee). *Fix a failure probability $\delta \in (0, 1)$ and an error tolerance $\varepsilon \in (0, 1)$. Let \mathbf{A} be any positive-semidefinite matrix; let \mathbf{S} be an index set of cardinality $|\mathbf{S}| = k$; and define $\mathbf{M} = \mathbf{A}(\mathbf{S}, :) \mathbf{A}(:, \mathbf{S}) + \mu \mathbf{A}(\mathbf{S}, \mathbf{S})$. Draw a random sparse sign embedding $\Phi \in \mathbb{R}^{d \times N}$ with column sparsity ζ and embedding dimension d satisfying*

$$\zeta = \mathcal{O}(\log(k/\delta)) \quad \text{and} \quad d = \mathcal{O}(k \log(k/\delta)). \quad (2.10)$$

With probability at least $1 - \delta$ over the randomness in Φ , the KRILL preconditioner $\mathbf{P} = \mathbf{A}(\mathbf{S}, :) \Phi^ \Phi \mathbf{A}(:, \mathbf{S}) + \mu \mathbf{A}(\mathbf{S}, \mathbf{S})$ controls the condition number at a level*

$$\kappa(\mathbf{P}^{-1/2} \mathbf{M} \mathbf{P}^{-1/2}) \leq 3. \quad (2.11)$$

Conditional on the event (2.11), when we apply preconditioned CG to the linear system $\mathbf{M} \hat{\beta} = \mathbf{A}(\mathbf{S}, :) \mathbf{y}$, we obtain an approximate solution $\hat{\beta}^{(t)}$ for which

$$\|\hat{\beta}^{(t)} - \hat{\beta}\|_{\mathbf{M}} \leq \varepsilon \|\hat{\beta}\|_{\mathbf{M}}, \quad (2.12)$$

at any iteration $t \geq \log(2/\varepsilon)$, where $\hat{\beta}$ is the actual solution.

Theorem 2.3 implies that KRILL can solve any restricted KRR problem in $\mathcal{O}((N + k^2)k \log k)$ operations. In contrast, FALKON-type preconditioners [30, 44, 45] are only guaranteed to solve restricted KRR problems if the number of centers and regularization satisfy $k = \Omega(\sqrt{N})$ and $\mu = \Omega(\sqrt{N})$ [44, 45]. Given these constraints, it is no surprise that KRILL performs more robustly than FALKON in our experiments.

Figure 6 evaluates KRILL’s capacity to control the conditioning of the 20 example problems when $\mu/N = 10^{-12}$. Before KRILL preconditioning, the condition numbers range from 10^1 – 10^{15} . After KRILL preconditioning, the condition numbers are concentrated in the range 10^1 – 10^2 . The

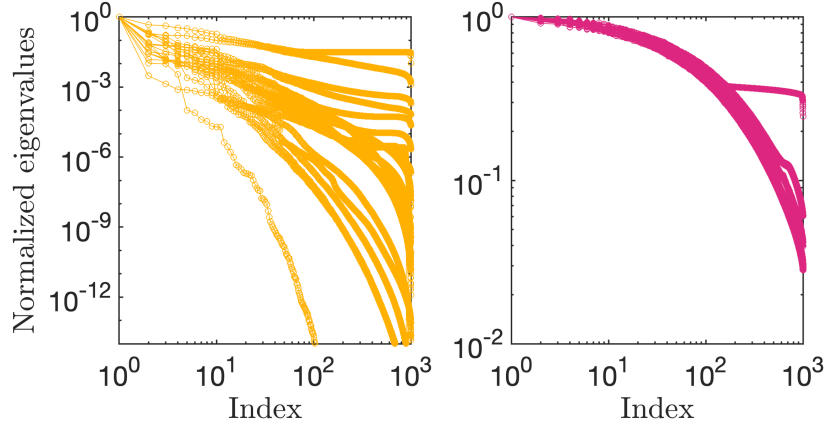


Figure 6: Eigenvalue decay for the 20 KRR problems in Table 1. Left panel shows normalized eigenvalues of the matrix $\mathbf{M} = \mathbf{A}(\mathbf{S}, :) \mathbf{A}(:, \mathbf{S}) + \mu \mathbf{A}(\mathbf{S}, \mathbf{S})$ before KRILL preconditioning (normalized by the largest eigenvalue). Right panel shows normalized eigenvalues of the matrix $\mathbf{P}^{-1/2} \mathbf{M} \mathbf{P}^{-1/2}$ after KRILL preconditioning.

preconditioned eigenvalues approximately align with one another, and they align with the inverse square singular values of a $2k \times k$ Gaussian matrix, which has the approximate condition number $(1 + (1/\sqrt{2})^2)/(1 - (1/\sqrt{2})^2) \approx 34.0$ (for intuition, see [37, Sec. 2]). This comparison shows that the performance of KRILL is largely independent of the details of the kernel matrix \mathbf{A} and only depends on the embedding dimension $d = 2k$.

3 Background and comparisons with other preconditioners

In this section, we compare our new preconditioners with existing preconditioners for solving the full-data and restricted KRR equations. To begin, we observe that the full-data and restricted KRR equations both take the form

$$\mathbf{M} \mathbf{z} = \mathbf{b}, \quad (3.1)$$

where $\mathbf{M} \in \mathbb{R}^{d \times d}$ is a positive-definite matrix and $\mathbf{b} \in \mathbb{R}^d$ is a vector. In full-data KRR, the dimension d equals the number of data points, $d = N$. In restricted KRR, the dimension equals the number of data centers, $d = k$.

Preconditioned conjugate gradient The conjugate gradient (CG) algorithm [46, §6.7] is a popular approach for solving linear systems of the form (3.1). When \mathbf{M} is well-conditioned ($\kappa(\mathbf{M}) \approx 1$), CG gives a high-accuracy solution using only a small number of iterations, with each iteration requiring a matrix–vector product with \mathbf{M} . More precisely, the following bound [46, eq. (6.128)] controls the convergence rate of the CG iterates $\mathbf{z}^{(0)}, \mathbf{z}^{(1)}, \dots$ to the solution \mathbf{z} of the system (3.1):

$$\|\mathbf{z}^{(t)} - \mathbf{z}\|_{\mathbf{M}} \leq 2 \left(\frac{\sqrt{\kappa(\mathbf{M})} - 1}{\sqrt{\kappa(\mathbf{M})} + 1} \right)^t \|\mathbf{z}^{(0)} - \mathbf{z}\|_{\mathbf{M}}, \quad (3.2)$$

The convergence is exponentially fast in the \mathbf{M} -norm $\|\mathbf{v}\|_{\mathbf{M}} := (\mathbf{v}^* \mathbf{M} \mathbf{v})^{1/2}$. However, the exponential rate depends on the condition number $\kappa(\mathbf{M})$, and it can be slow when $\kappa(\mathbf{M})$ is large.

The full-data and restricted KRR equations are typically ill-conditioned, so we need to apply a positive-definite preconditioner $\mathbf{P} \in \mathbb{R}^{d \times d}$ to these problems to improve the convergence. The

Algorithm 3 Preconditioned conjugate gradient

Input: Subroutine `Product` computing the action $\mathbf{u} \mapsto \mathbf{M}\mathbf{u}$, subroutine `Preconditioner` computing the action $\mathbf{u} \mapsto \mathbf{P}^{-1}\mathbf{u}$, right-hand-side vector $\mathbf{b} \in \mathbb{R}^N$, and tolerance ε .

Output: Approximate solution β_\star to $\mathbf{M}\beta = \mathbf{b}$.

- 1: Initialize $\beta_\star \leftarrow \mathbf{0}$, $\mathbf{r} \leftarrow \mathbf{b}$, $\mathbf{z} \leftarrow \text{Preconditioner}(\mathbf{r})$, $\mathbf{p} \leftarrow \mathbf{z}$, and $\omega \leftarrow \mathbf{z}^*\mathbf{r}$
 - 2: **while** $\|\mathbf{r}\| \geq \varepsilon \cdot \|\mathbf{b}\|$ **do**
 - 3: $\mathbf{v} \leftarrow \text{Product}(\mathbf{p})$
 - 4: $\eta \leftarrow \omega/\mathbf{v}^*\mathbf{p}$, $\beta_\star \leftarrow \beta_\star + \eta\mathbf{p}$, $\mathbf{r} \leftarrow \mathbf{r} - \eta\mathbf{v}$
 - 5: $\mathbf{z} \leftarrow \text{Preconditioner}(\mathbf{r})$
 - 6: $\omega_{\text{new}} \leftarrow \mathbf{z}^*\mathbf{r}$, $\gamma \leftarrow \omega_{\text{new}}/\omega$, $\omega \leftarrow \omega_{\text{new}}$
 - 7: $\mathbf{p} \leftarrow \mathbf{z} + \gamma\mathbf{p}$
 - 8: **end while**
-

preconditioned CG algorithm (Algorithm 3, described in [24, §10.3]), is equivalent to applying standard CG to the preconditioned system

$$(\mathbf{P}^{-1/2}\mathbf{M}\mathbf{P}^{-1/2})(\mathbf{P}^{1/2}\mathbf{z}) = \mathbf{P}^{-1/2}\mathbf{b}.$$

The convergence rate of preconditioned CG no longer depends on $\kappa(\mathbf{M})$, instead depending on $\kappa(\mathbf{P}^{-1/2}\mathbf{M}\mathbf{P}^{-1/2})$. Fast convergence occurs when $\mathbf{P} \approx \mathbf{M}$.

In the rest of this section, we review the history of preconditioned CG methods for the full-data and restricted KRR equations. We do not cover KRR methods based on sketch-and-solve [1, 6] or stochastic gradient descent [17, 28], since the accuracy of these methods is more limited [29, §10].

3.1 Preconditioners for full-data KRR

To efficiently solve the full-data KRR problem $(\mathbf{A} + \mu\mathbf{I})\mathbf{x} = \mathbf{y}$, we can apply a preconditioner of the form

$$\mathbf{P} = \hat{\mathbf{A}} + \mu\mathbf{I},$$

where $\hat{\mathbf{A}} \in \mathbb{R}^{N \times N}$ is an approximation of the full kernel matrix \mathbf{A} . Ideally, we would obtain an accurate approximation $\hat{\mathbf{A}} \approx \mathbf{A}$, and we would quickly apply \mathbf{P}^{-1} to a vector at every CG step.

In the KRR literature, $\hat{\mathbf{A}}$ is typically constructed as a low-rank approximation of \mathbf{A} [5, 16, 22, 23, 53]. A low-rank approximation can only be accurate when the kernel matrix is close to being low-rank, i.e., when the eigenvalues of \mathbf{A} decay quickly. However, even under favorable eigenvalue decay conditions, it has been a challenge to identify accurate and computationally tractable low-rank approximations.

A popular low-rank approximation method for KRR problems is the *column Nyström approximation* [29, §19.2], which is obtained from a partial Cholesky decomposition with pivoting. The column Nyström approximation takes the form

$$\hat{\mathbf{A}} = \mathbf{A}(:, \mathbf{S})\mathbf{A}(\mathbf{S}, \mathbf{S})^\dagger\mathbf{A}(\mathbf{S}, :), \quad (3.3)$$

where $\mathbf{S} = \{s_1, s_2, \dots, s_r\}$ coincides with the pivots chosen in the Cholesky procedure, and it lists the columns of \mathbf{A} that participate in the approximation. The column Nyström approximation is convenient because it is formed from the columns of \mathbf{A} indexed by \mathbf{S} and does not require viewing the rest of the matrix. Yet the accuracy of the column Nyström approximation depends on selecting a good index set \mathbf{S} . In the context of full-data KRR, there are two prominent strategies for picking the set \mathbf{S} of columns in the Nyström approximation, called uniform sampling and greedy selection. Both of these approaches exhibit serious failure modes.

Algorithm 4 Blocked RPCHOLESKY for psd low-rank approximation

Input: Positive semidefinite matrix $\mathbf{A} \in \mathbb{R}^{N \times N}$, approximation rank k , block size B .

Output: Factor matrix $\mathbf{F} \in \mathbb{R}^{N \times k}$, index set \mathbf{S} .

```

1: Initialize  $\mathbf{F} \leftarrow \mathbf{0}_{N \times k}$ ,  $\mathbf{S} \leftarrow \emptyset$ ,  $\mathbf{d} \leftarrow \text{diag}(\mathbf{A})$ ,  $i \leftarrow 0$ 
2: while  $i < k$  do
3:   Sample iid indices  $s_1, \dots, s_{\min\{B, k-i\}} \sim \mathbf{d}/\text{SUM}(\mathbf{d})$ 
4:    $\mathbf{S}' \leftarrow \text{UNIQUE}(s_1, \dots, s_{\min\{B, k-i\}})$ ,  $\mathbf{S} \leftarrow \mathbf{S} \cup \mathbf{S}'$ 
5:    $\mathbf{G} \leftarrow \mathbf{A}(:, \mathbf{S}') - \mathbf{F}(:, 1:i) \mathbf{F}(\mathbf{S}', 1:i)^*$ 
6:    $\mathbf{R} \leftarrow \text{CHOLESKY}(\mathbf{G}(\mathbf{S}', :))$   $\triangleright \mathbf{G}(\mathbf{S}', :) = \mathbf{R}^* \mathbf{R}$ 
7:    $\mathbf{F}(:, (i+1) : (i+|\mathbf{S}'|)) \leftarrow \mathbf{G} \mathbf{R}^{-1}$ 
8:    $\mathbf{d} \leftarrow \mathbf{d} - \text{SQUAREDROWNORMS}(\mathbf{F}(:, (i+1) : (i+|\mathbf{S}'|)))$ 
9:    $i \leftarrow i + |\mathbf{S}'|$ 
10: end while

```

Failure of uniform sampling The first strategy selects the column pivots s_1, \dots, s_r uniformly at random [16, 22]. This *uniform sampling* method can be effective for some problems, but it fails to explore less populated regions of data space. To illustrate this shortcoming, let $\mathbf{1}_m$ denote the m -vector with entries equal to 1, and consider the kernel matrix

$$\mathbf{A} = \begin{pmatrix} \mathbf{1}_{N-N^{1/3}} \mathbf{1}_{N-N^{1/3}}^* & \\ & \mathbf{1}_{N^{1/3}} \mathbf{1}_{N^{1/3}}^* \end{pmatrix}.$$

In principle, constructing a preconditioner for \mathbf{A} should be easy, since the μ -tail rank (Definition 2.1) is just $\text{rank}_\mu(\mathbf{A}) = 2$ for any $\mu < N^{1/3}$. However, uniform sampling selects many columns from the left block and neglects columns from the right block that are also needed to ensure the approximation quality. For uniform sampling to build an effective preconditioner, we need an approximation rank much higher than 2 and at least as large as $r = \Omega(N^{2/3})$.

Failure of greedy selection A second strategy for choosing columns is the *greedy selection* method [23, 53], in which we adaptively select each column pivot s_i by finding the largest diagonal element of the residual matrix $\mathbf{A} - \widehat{\mathbf{A}}_{(i-1)}$ after $i-1$ steps of the Cholesky procedure. The greedy method has the opposite failure mode from the uniform method: it focuses on outlier data points and fails to explore highly populated regions of data space. To see this limitation, let $\mathbf{I}_{N^{2/3}}$ denote the $N^{2/3} \times N^{2/3}$ identity matrix, and consider the kernel matrix

$$\mathbf{A} = \mathbf{1}_N \mathbf{1}_N^* + \begin{pmatrix} \frac{\delta}{2} \mathbf{1}_{N-N^{2/3}} \mathbf{1}_{N-N^{2/3}}^* & \\ & \delta \mathbf{I}_{N^{2/3}} \end{pmatrix}$$

for a small parameter $\delta > 0$. Constructing a preconditioner for \mathbf{A} is easy in theory, since $\text{rank}_\mu(\mathbf{A}) \leq 2$ for any $\mu \geq N^{2/3} \delta$. Yet the greedy strategy selects columns from the right block first and misses the left columns. To provide an effective preconditioner, greedy sampling needs an approximation rank $r > N^{2/3}$, which is large enough that all the columns in the right block have been selected.

Advantages of RPCholesky In this paper, we propose a new KRR preconditioner that uses RPCHOLESKY (see Algorithm 4 or [12]) to select the columns for the Nyström approximation. In RPCHOLESKY, we adaptively sample the column pivot s_i with probability proportional to the diagonal entries of the residual matrix $\mathbf{A} - \widehat{\mathbf{A}}_{(i-1)}$ after $i-1$ steps of the Cholesky procedure.

Because of the adaptive sampling distribution, RPCHOLESKY balances exploration of the small diagonal entries and exploitation of the large diagonal entries, avoiding the failure modes of both the uniform and greedy strategies. RPCHOLESKY is guaranteed to produce an effective preconditioner if the approximation rank r is set to a modest multiple of the μ -tail rank (Theorem 2.2).

Ridge leverage score sampling *Ridge leverage score sampling* [1, 36, 45] is a more elaborate procedure for selecting the pivots in the Nyström approximation. This method first approximates the ridge leverage scores, which are the diagonal entries $\ell^\lambda = \text{diag}(\mathbf{A}(\mathbf{A} + \lambda\mathbf{I})^{-1})$ for a parameter $\lambda > 0$. Then, the method randomly generates a Nyström approximation whose pivots are selected with probabilities proportional to the ridge leverage scores. While RLS sampling can lead to an approximation that is nearly as accurate as RPCHOLESKY (see Figure 1), it can also produce lower-quality approximations given challenging inputs [12]. Additionally, RLS sampling is slower than the blocked implementation of RPCHOLESKY given in Algorithm 4, because of the requirement to approximate the ridge leverage scores. For example, when we apply RLS sampling (with the RecursiveRLS algorithm [36]) to compute a rank-1000 approximation of a kernel matrix of size $N = 4 \times 10^4$, the runtime is $2.3\times$ slower than RPCHOLESKY’s runtime.

More expensive Gaussian preconditioner A different type of preconditioner for full-data KRR is based on the *Gaussian Nyström approximation* [22]

$$\hat{\mathbf{A}} = \mathbf{A}\mathbf{X}(\mathbf{X}^*\mathbf{A}\mathbf{X})^\dagger\mathbf{X}^*\mathbf{A},$$

where $\mathbf{X} \in \mathbb{R}^{N \times r}$ is a matrix with independent standard normal entries. Forming the Gaussian Nyström approximation requires r matrix–vector multiplications with the full kernel matrix, which is much more expensive than forming a column Nyström approximation (3.3) in factored form. To maintain a cost of $\mathcal{O}(N^2)$ operations, we can only run Gaussian Nyström with a constant approximation rank $r = \mathcal{O}(1)$, whereas we can run RPCHOLESKY preconditioning with a larger approximation rank $r = \mathcal{O}(\sqrt{N})$. Because of this larger approximation rank, RPCHOLESKY preconditioning leads to a more accurate approximation with stronger theoretical guarantees.

Other approaches We briefly mention two other types of approximations that can be used to build preconditioners for the full-data KRR problem. First, certain types of kernel matrices can be approximated using *random features* [5, 16], but the quality of the approximation tends to be poor. Numerical tests indicate that the random features approach does not yield a competitive preconditioner [16, 55]. See Figures 1 and 2 for further numerical results. Second, the kernel matrix can also be approximated using a hierarchical low-rank approximation [3, 11, 16, 56]. The hierarchical approach has mainly been applied to low-dimensional input data, and the applicability to high-dimensional data sets remains unclear [3].

3.2 Preconditioners for restricted KRR

To efficiently solve the restricted KRR problem $[\mathbf{A}(\mathbf{S}, :)\mathbf{A}(:, \mathbf{S}) + \mu\mathbf{A}(\mathbf{S}, \mathbf{S})] \hat{\boldsymbol{\beta}} = \mathbf{A}(\mathbf{S}, :)\mathbf{y}$, we can apply a preconditioner of the form

$$\mathbf{P} = \hat{\mathbf{G}} + \mu\mathbf{A}(\mathbf{S}, \mathbf{S}). \tag{3.4}$$

where $\hat{\mathbf{G}} \in \mathbb{R}^{k \times k}$ approximates the Gram matrix $\mathbf{G} = \mathbf{A}(\mathbf{S}, :)\mathbf{A}(:, \mathbf{S})$.

Algorithm 5 Sparse sign embedding

Input: Embedding dimension d , input dimension N , sparsity level ζ .

Output: Embedding matrix $\Phi \in \mathbb{R}^{d \times N}$ in sparse (e.g., CSR) format.

1: $\mathbf{rows} \leftarrow \mathbf{0}_{\zeta N}, \mathbf{cols} \leftarrow \mathbf{0}_{\zeta N}, \mathbf{vals} \leftarrow \mathbf{0}_{\zeta N}$

2: **for** $1 \leq j \leq N$ **do**

3: $\mathbf{rows}((j-1)\zeta+1 : j\zeta) \leftarrow$ distinct uniformly random indices from $\{1, \dots, d\}$

4: $\mathbf{cols}((j-1)\zeta+1 : j\zeta) \leftarrow j$

5: $\mathbf{vals}((j-1)\zeta+1 : j\zeta) \leftarrow \zeta^{-1/2} \cdot \text{UNIF}\{\pm 1\}^\zeta$

6: **end for**

7: $\Phi \leftarrow \text{SPARSE}(\mathbf{rows}, \mathbf{cols}, \mathbf{vals}, d, N)$

$\triangleright d \times N$ sparse matrix with specified entries

FALKON, the current state-of-the-art FALKON-type preconditioners [30, 44, 45] are based on a Monte Carlo approximation of \mathbf{G} . The Monte Carlo approach assumes that each data point $\mathbf{x}^{(i)}$ is selected as a center with nonzero probability $p_i = \mathbb{P}\{i \in \mathbf{S}\}$. The Gram matrix is then approximated as

$$\hat{\mathbf{G}} = \mathbf{A}(\mathbf{S}, \mathbf{S})\mathbf{D}(\mathbf{S}, \mathbf{S})^{-1}\mathbf{A}(\mathbf{S}, \mathbf{S}), \quad (3.5)$$

where $\mathbf{D} = \text{diag}(p_1, p_2, \dots, p_N)$ is the diagonal matrix of the selection probabilities. The matrix entries g_{ij} and \hat{g}_{ij} can be explicitly written as

$$g_{ij} = \sum_{\ell=1}^N a_{s_i, \ell} a_{\ell, s_j} \quad \text{and} \quad \hat{g}_{ij} = \sum_{\ell=1}^N \frac{\mathbb{1}\{\ell \in \mathbf{S}\}}{p_\ell} a_{s_i, \ell} a_{\ell, s_j}.$$

These entries are clearly linked together in expectation:

$$\sum_{\ell=1}^N a_{i, \ell} a_{\ell, j} = \mathbb{E} \left[\sum_{\ell=1}^N \frac{\mathbb{1}\{\ell \in \mathbf{S}\}}{p_\ell} a_{i, \ell} a_{\ell, j} \right] \quad \text{for fixed indices } 1 \leq i, j \leq N,$$

which suggests that the quantities g_{ij} and \hat{g}_{ij} will be close under appropriate conditions. FALKON [30, 44] is a special case of (3.5) in which the centers are sampled uniformly at random, and FALKON-BLESS [45] is a special case of (3.5) in which the centers are chosen by ridge leverage score sampling.

The main limitation of FALKON-type preconditioners is the large size of the Monte Carlo approximation error. To account for the Monte Carlo error, the available analyses [44, 45] assume a large number of centers $k = \Omega(\sqrt{N})$ and a large regularization $\mu = \Omega(\sqrt{N})$. When these assumptions are satisfied, FALKON-type preconditioners solve the restricted KRR equations in $\mathcal{O}((N + k^2)k)$ operations. However, the assumptions on k and μ may not be satisfied in practice. For example, μ is often small when chosen by cross-validation, and [44] contains examples of μ values up to five orders of magnitude smaller than $\mu = \sqrt{N}$.

Block Lanczos preconditioner A different preconditioner suggested by [25] approximates the Gram matrix \mathbf{G} using the randomized block Lanczos algorithm [35]. Block Lanczos produces a high-quality rank- r approximation in $\mathcal{O}(Nkr \log k)$ arithmetic operations. The preconditioner can be quite effective when the \mathbf{G} has rapidly decaying eigenvalues and $r = \mathcal{O}(1)$, but the general case requires setting $r = \mathcal{O}(k)$, which is comparatively very expensive. A block-Lanczos-based preconditioner led to slow convergence in the numerical experiments of [38], suggesting that the approach is unlikely to be competitive with KRILL for challenging problems.

KRILL In this paper, we recommend using a more accurate approximation,

$$\widehat{\mathbf{G}} = \mathbf{A}(\mathbf{S}, :) \Phi^* \Phi \mathbf{A}(:, \mathbf{S}),$$

where $\Phi \in \mathbb{R}^{d \times N}$ is a sparse random sign embedding (see Algorithm 5 or [15]). With this approximation, we can guarantee the effectiveness of the KRILL preconditioner $\mathbf{P} = \widehat{\mathbf{G}} + \mu \mathbf{A}(\mathbf{S}, \mathbf{S})$, regardless of the number of centers k and the regularization μ .

KRILL is inspired by the *sketch-and-precondition* approach for solving overdetermined least-squares problems [29, §10.5]. In sketch-and-precondition, we use a random embedding to approximate the matrix appearing in the normal equations, and the approximate matrix serves as a preconditioner for solving the least-squares problem. Sketch-and-precondition was first proposed in [42] and later refined in [4, 14, 26, 31, 33]. It has been applied with several different embeddings [29, §§8–9], but the empirical comparisons of [19, Fig. 1] suggest the sparse sign embedding is the most efficient.

KRILL differs from classical presentations of sketch-and-precondition because the embedding is applied to the Gram matrix term $\mathbf{A}(:, \mathbf{S}) \mathbf{A}(\mathbf{S}, :)$ but not the regularization term $\mu \mathbf{A}(\mathbf{S}, \mathbf{S})$. This idea of “partial sketching” appears in [34, 39], and it improves the accuracy of the approximation. Notwithstanding this difference, KRILL is motivated by the same ideas and its analysis follows the same patterns as classical sketch-and-precondition.

4 Case studies

In this section, we apply our preconditioning strategies to two scientific applications. In Section 4.1, we apply full-data KRR with RPCHOLESKY preconditioning to predict the chemical properties of a wide range of molecules. In Section 4.2, we apply restricted KRR with KRILL preconditioning to distinguish exotic particle collisions from a background process.

4.1 HOMO energy prediction

A major goal of chemical machine learning is to search over a large parameter space of molecules and identify candidate molecules which may possess useful properties [18, 54]. To support this goal, scientists have assembled the QM9 data set, which describes the properties of 1.3×10^5 organic molecules [41, 43]. Although the QM9 data set is generated by relatively expensive (and highly repetitive) density functional theory calculations, we can use the QM9 data to train machine learning models that efficiently make out-of-sample predictions, limiting the need for density functional theory in the future. Ideally, machine learning would identify a small collection of promising molecules, which scientists could then analyze and test.

A recent journal article [49], which was selected as an editor’s pick in the Journal of Chemical Physics, describes the difficulties in applying KRR to the QM9 data set. The authors aim to predict the highest-occupied-molecular-orbital (HOMO) energy. In their simplest approach, they make HOMO predictions based on the *Coulomb matrix* representation of molecules, which is a set of features based on the distances between the atomic nuclei and the nuclear charges. After defining the features, they standardize the features and apply an ℓ_1 Laplace kernel

$$K(\mathbf{x}, \mathbf{x}') = \exp\left(-\frac{1}{\sigma} \|\mathbf{x} - \mathbf{x}'\|_{\ell_1}\right),$$

with a bandwidth σ and a ridge parameter μ chosen using cross-validation.

Given the moderate size of the QM9 data set ($N = 1.3 \times 10^5$), it takes just a few seconds to load the data and form individual columns of the kernel matrix. However, on a laptop-scale computer (64GB RAM), there is not enough working memory to store or factorize the complete kernel matrix.

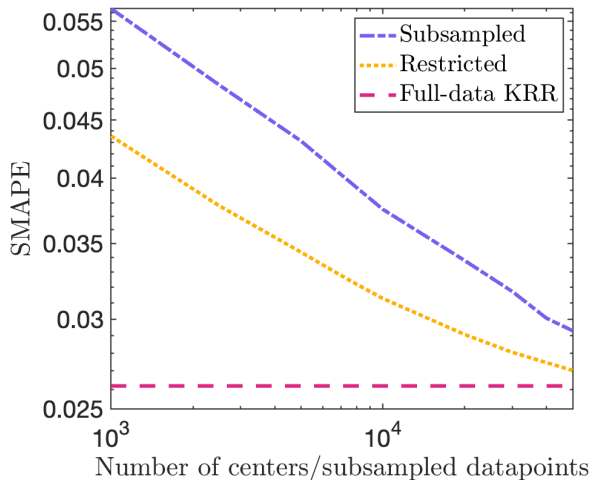


Figure 7: SMAPE versus number of centers / number of subsampled data points for the HOMO energy prediction problem ($N = 10^5$).

The authors of [49] address these computational constraints by randomly subsampling $N = 32,000$ or fewer data points and applying full-data KRR to the random sample. In their Fig. 8, they show that the predictive accuracy improves by a factor of $2\times$ as they increase the size of the data from $N = 1,000$ to $N = 32,000$ data points. Even with $N = 32,000$ data points, the predictive accuracy does not saturate, and thus computational constraints are limiting the predictive accuracy of the KRR model.

Building on this work, we can apply KRR to *the complete QM9 data set* either using (i) restricted KRR or (ii) full-data KRR with RPCHOLESKY preconditioning. In all our experiments, we split the data into $N = 10^5$ training points and $M = 3 \times 10^4$ test points, and we measure the predictive accuracy using the symmetric mean absolute percentage error (SMAPE):

$$\text{SMAPE}(\hat{\mathbf{y}}, \mathbf{y}) = \frac{1}{M} \sum_{i=1}^M \frac{|\hat{y}_i - y_i|}{(|\hat{y}_i| + |y_i|)/2}. \quad (4.1)$$

The results are presented in Figures 7 to 9.

Restricted KRR is a relatively cheap approach for predicting HOMO energies with the QM9 data set, since we can store the $k \times k$ preconditioner and $N \times k$ kernel submatrix in working memory with up to $k = 50,000$ centers. Figure 7 shows that restricted KRR is more accurate than randomly subsampling the data and applying full-data KRR to the random sample. Still, the predictive accuracy increases with the number of centers k and does not saturate even when $k = N/2$.

Full-data KRR is the most accurate approach for predicting HOMO energies, but it relies on repeated matrix–vector multiplication with the full kernel matrix. Since the kernel matrix is too large to store in 64GB of working memory, we can only store one block of the matrix at a time and perform the multiplications in a block-wise fashion. Each multiplication requires tens of minutes of computing, due to the cost of evaluating the kernel matrix each time the entries are needed. The training of the full-data KRR model is very slow unless we find a preconditioner that controls the total number of CG iterations.

Figure 8 compares several preconditioning strategies for full-data KRR. The worst strategy is unpreconditioned CG, which leads to no perceivable convergence over the first 100 iterations. Uniform and greedy Nyström preconditioning (with approximation rank $r = 10^3$) improve the

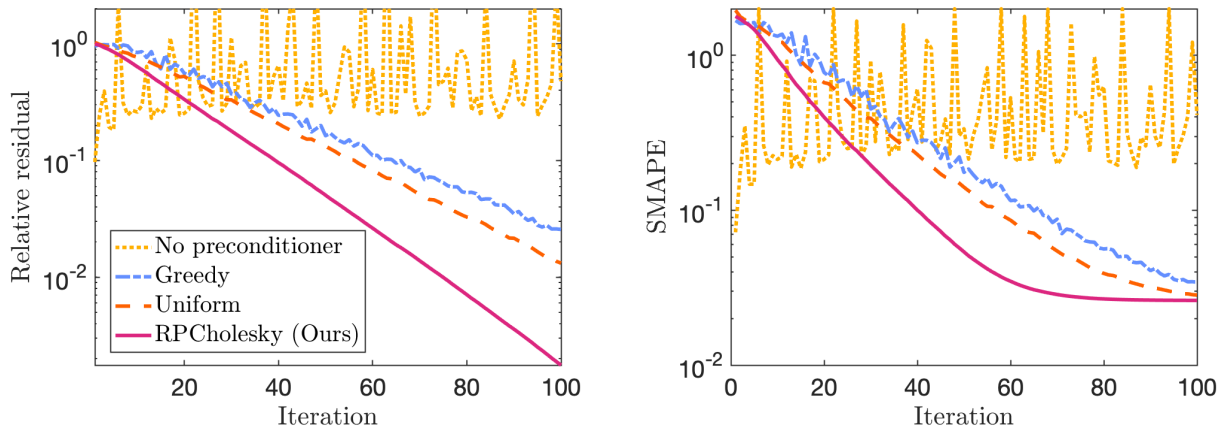


Figure 8: (*left*) Relative residual $\|(\mathbf{A} + \mu\mathbf{I})\boldsymbol{\beta} - \mathbf{y}\| / \|\mathbf{y}\|$ and (*right*) SMAPE for different column Nyström preconditioners for the HOMO energy prediction task

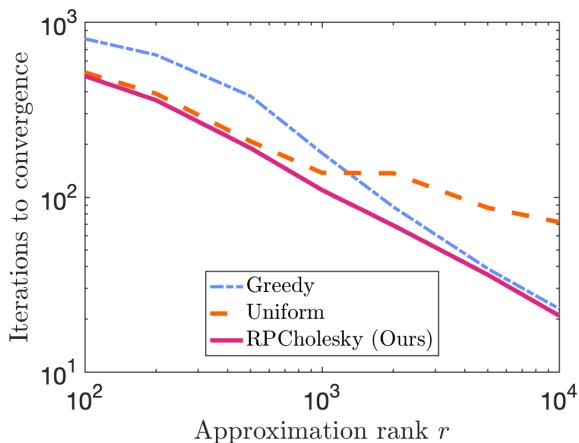


Figure 9: Number of CG iterations to achieve a relative residual of $\varepsilon < 10^{-3}$ with RPCHOLESKY preconditioning for the HOMO energy prediction task.

convergence speed, but they still require 100 or more iterations for the predictive accuracy to saturate. RPCHOLESKY (also with $r = 10^3$) is the fastest method, leading to converged accuracy after 60 iterations.

Figure 9 shows that we can reduce the total number of CG iterations even further, by a factor of $5\times$, if we increase the RPCHOLESKY approximation rank from $r = 10^3$ to $r = 10^4$. However, we also need to consider the cost of preparing the preconditioner, which requires $\mathcal{O}(Nr^2)$ operations. To achieve an appropriate balance, we recommend tuning the value of r based on computational constraints, and r should typically be small enough that the preconditioner can be stored in working memory. For example, an intermediate value of $10^3 < r < 10^4$ would be most appropriate for the HOMO energy prediction problem given our computing architecture.

Figure 9 shows a curious trend in which RPCHOLESKY performs similarly to uniform pivot selection for a small approximation rank ($r < 500$) and performs similarly to greedy pivot selection for a large approximation rank ($r > 5000$). It is an open question to identify the problems and approximation ranks for which uniform or greedy pivot selection are as successful as RPCHOLESKY.

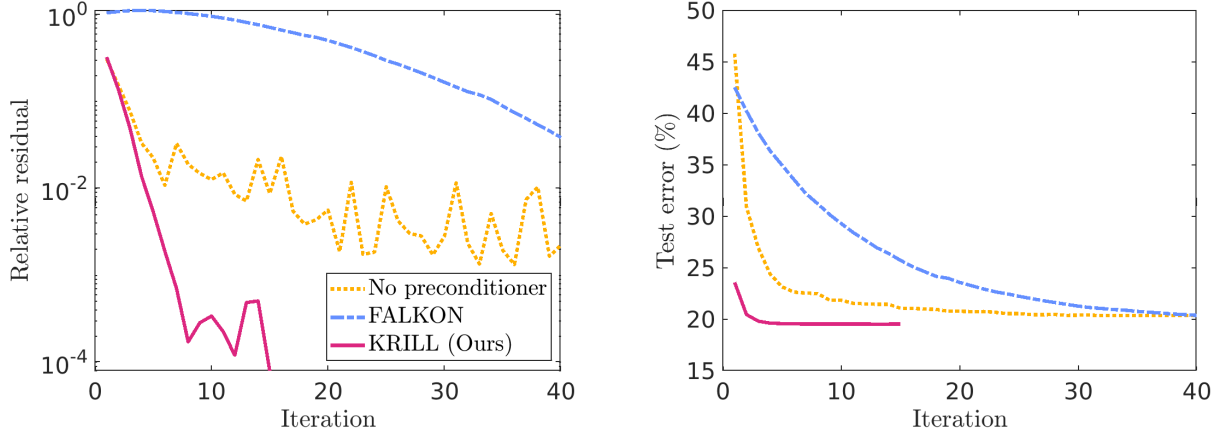


Figure 10: (left) Relative residual $\|(\mathbf{A}(\mathbf{S}, :) \mathbf{A}(:, \mathbf{S}) + \mu \mathbf{A}(\mathbf{S}, \mathbf{S})) \hat{\boldsymbol{\beta}} - \mathbf{A}(\mathbf{S}, :) \mathbf{y}\| / \|\mathbf{A}(\mathbf{S}, :) \mathbf{y}\|$ and (right) test error for FALKON vs. KRILL for the SUSY classification problem

4.2 Exotic particle detection

The Large Hadron Collider (LHC) is a particle accelerator that is being used to search for exotic particles not included in the standard model of physics. Each second, the LHC collides roughly one billion proton–proton pairs and produces one petabyte of data. Yet, exotic particles are believed to be produced in fewer than one per billion collisions, so only a small fraction of the data is relevant and the LHC is increasingly relying on machine learning to identify the most important observations for testing exotic particle models [40].

To help train machine learning algorithms, Baldi, Sadowsky, and Whiteson [7] have produced the SUSY data set ($N = 5 \times 10^6$) from Monte Carlo simulations of the decay processes of standard model bosons and supersymmetric particles not included in the standard model. Following [27, 44, 45], we will apply restricted KRR to the SUSY data to distinguish between the bosonic and supersymmetric decay processes.

For our KRR application, we split the data into $N = 4.5 \times 10^6$ training data points and $M = 5 \times 10^5$ testing data points, and we select $k = 10^4$ data centers uniformly at random. Then we standardize the data features and apply a squared exponential kernel (2.3) with bandwidth $\sigma = 4$. The parameters k and σ are the same ones used in previous work [44, 45], but we use a smaller regularization $\mu/N = 2 \times 10^{-10}$ (compared to $\mu/N = 10^{-6}$ in [27, 44, 45]) which improves the test error from 19.6% to 19.5%. We apply KRILL, FALKON, and unpreconditioned CG to solve the restricted KRR equations with these parameter choices. We terminate after forty iterations or when the relative residual falls below $\varepsilon = 10^{-4}$, leading to the results in Figures 10 and 11.

Figure 10 demonstrates the superior performance of KRILL, which reaches a test error of 19.5% after just four iterations. Meanwhile, unpreconditioned CG fails to achieve such a low test error after forty iterations, and FALKON converges even more slowly than unpreconditioned CG. One reason for the slow convergence of FALKON is the small regularization parameter $\mu/N = 2 \times 10^{-10}$, which is a known failure mode for the preconditioner [27, Sec. 3]. Indeed, a previous application [45] of FALKON to the SUSY data set with a larger regularization $\mu/N = 10^{-6}$ achieved test error convergence more quickly, in just twenty iterations (still five times slower than KRILL). A major advantage of KRILL is the reliable performance for the full range of μ values, which empowers users to choose the regularization that gives the lowest test error.

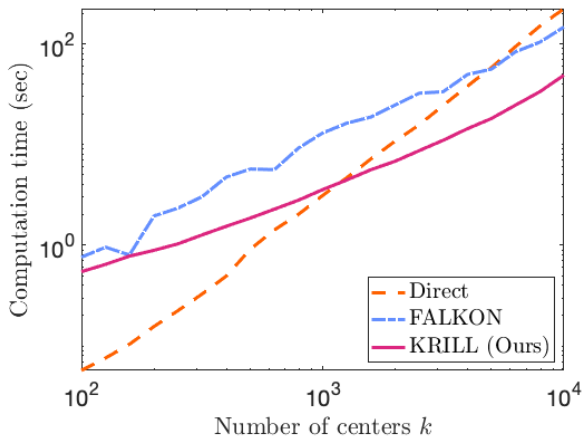


Figure 11: Runtime versus number of centers for the SUSY classification problem ($N = 5 \times 10^5$).

Last, Figure 11 evaluates the total computation time needed to form the preconditioner and solve the restricted KRR equations up to a relative residual of $\varepsilon = 10^{-4}$. For this figure, we randomly subsample $N = 5 \times 10^5$ data points so that the kernel submatrix fits in 64GB of working memory, and we compare KRILL, FALKON, and the direct method of forming and inverting $\mathbf{A}(\mathbf{S}, :) \mathbf{A}(:, \mathbf{S}) + \mu \mathbf{A}(\mathbf{S}, \mathbf{S})$. We find that KRILL is the dominant algorithm once the number of centers reaches $k = 1250$. KRILL outperforms the direct method because of the superior $\mathcal{O}((N + k^2)k)$ computational cost, and KRILL outperforms FALKON because it converges in roughly $4 \times$ fewer CG iterations. As an advantage, the direct method is solving the restricted KRR equations up to machine precision, whereas KRILL and FALKON are only solving the equations up to a relative residual of $\varepsilon = 10^{-4}$. Nonetheless, the test error plateaus at a threshold of $\varepsilon = 10^{-4}$ in all our experiments.

5 Theoretical results

In this section, we prove our main theoretical results, Theorems 2.2 and 2.3.

5.1 Proof of Theorem 2.2

Let $\hat{\mathbf{A}}$ be a Nystrom approximation of the psd matrix \mathbf{A} , and set $\mathbf{P} = \hat{\mathbf{A}} + \mu \mathbf{I}$. As the first step of our proof, we will show that

$$\kappa(\mathbf{P}^{-1/2}(\mathbf{A} + \mu \mathbf{I})\mathbf{P}^{-1/2}) \leq 1 + \text{tr}(\mathbf{A} - \hat{\mathbf{A}})/\mu. \quad (5.1)$$

To that end, observe that $\mathbf{P} \preceq \mathbf{A} + \mu \mathbf{I}$, because the Nyström approximation $\hat{\mathbf{A}}$ is bounded from above by \mathbf{A} . By conjugation with $\mathbf{P}^{-1/2}$, we obtain

$$\mathbf{I} \preceq \mathbf{P}^{-1/2}(\mathbf{A} + \mu \mathbf{I})\mathbf{P}^{-1/2}$$

and thus

$$1 \leq \lambda_{\min}(\mathbf{P}^{-1/2}(\mathbf{A} + \mu \mathbf{I})\mathbf{P}^{-1/2}). \quad (5.2)$$

Next, a short calculation shows that

$$\mathbf{P}^{-1/2}(\mathbf{A} + \mu \mathbf{I})\mathbf{P}^{-1/2} = \mathbf{I} + \mathbf{P}^{-1/2}(\mathbf{A} - \hat{\mathbf{A}})\mathbf{P}^{-1/2}.$$

Since the spectral norm is submultiplicative and equals the largest eigenvalue of a psd matrix, we deduce that

$$\begin{aligned}\lambda_{\max}(\mathbf{P}^{-1/2}(\mathbf{A} + \mu\mathbf{I})\mathbf{P}^{-1/2}) &= 1 + \lambda_{\max}(\mathbf{P}^{-1/2}(\mathbf{A} - \widehat{\mathbf{A}})\mathbf{P}^{-1/2}) \\ &\leq 1 + \|\mathbf{P}^{-1/2}\|^2 \|\mathbf{A} - \widehat{\mathbf{A}}\| = 1 + \|\mathbf{P}^{-1}\| \|\mathbf{A} - \widehat{\mathbf{A}}\|.\end{aligned}$$

Last, using the fact that $\|\mathbf{A} - \widehat{\mathbf{A}}\| \leq \text{tr}(\mathbf{A} - \widehat{\mathbf{A}})$ and $\lambda_{\min}(\mathbf{P}) \geq \mu$, we find

$$\lambda_{\max}(\mathbf{P}^{-1/2}(\mathbf{A} + \mu\mathbf{I})\mathbf{P}^{-1/2}) \leq 1 + \text{tr}(\mathbf{A} - \widehat{\mathbf{A}})/\mu. \quad (5.3)$$

Combining the bound (5.2) for the minimum eigenvalue with the bound (5.3) for the maximum eigenvalue verifies the condition number bound (5.1).

As our next step, we apply the main RPCHOLESKY error bound [12, Thm. 3.1] with rank $r = \text{rank}_{\mu}(\mathbf{A})$ and approximation accuracy $1 + \varepsilon = 2$, which guarantees

$$\mathbb{E} \text{tr}(\mathbf{A} - \widehat{\mathbf{A}}) \leq 2 \sum_{i > \text{rank}_{\mu}(\mathbf{A})} \lambda_i(\mathbf{A}) \quad (5.4)$$

for any r satisfying

$$r \geq \text{rank}_{\mu}(\mathbf{A}) (1 + \log(\text{tr} \mathbf{A} / \mu)).$$

The right-hand side of (5.4) is bounded by 2μ because of Definition 2.1 of the μ -tail rank of \mathbf{A} . Hence, combining (5.4) with the condition number bound (5.1) guarantees

$$\mathbb{E} \kappa(\mathbf{P}^{-1/2}(\mathbf{A} + \mu\mathbf{I})\mathbf{P}^{-1/2}) \leq 3.$$

By Markov's inequality, it follows that

$$\kappa(\mathbf{P}^{-1/2}(\mathbf{A} + \mu\mathbf{I})\mathbf{P}^{-1/2}) \leq 3/\delta$$

with failure probability at most δ . We apply the CG error bound (3.2) to obtain

$$\frac{\|\boldsymbol{\beta}^{(t)} - \boldsymbol{\beta}\|_{\mathbf{A} + \mu\mathbf{I}}}{\|\boldsymbol{\beta}\|_{\mathbf{A} + \mu\mathbf{I}}} \leq 2 \left(\frac{\sqrt{3/\delta} - 1}{\sqrt{3/\delta} + 1} \right)^t \leq 2e^{-2t\sqrt{\delta/3}} \leq 2e^{-t\sqrt{\delta}}$$

for each $t \geq 0$, with failure probability at most δ , which is equivalent to the stated convergence guarantee for RPCHOLESKY preconditioning. \square

5.2 Proof of Theorem 2.3

Cohen [15, Thm. 4.2] showed that a sparse sign embedding with parameters $d = \mathcal{O}(k \log(k/\delta))$ and $\zeta = \mathcal{O}(\log(k/\delta))$ satisfies the following oblivious subspace embedding property: for any k -dimensional subspace $\mathbf{X} \subseteq \mathbb{R}^N$, there is probability at least $1 - \delta$ that

$$(1/2) \|\mathbf{v}\|^2 \leq \|\Phi \mathbf{v}\|^2 \leq (3/2) \|\mathbf{v}\|^2 \quad \text{for every } \mathbf{v} \in \mathbf{X}. \quad (5.5)$$

We set $\mathbf{X} = \text{range}(\mathbf{A}(:, \mathbf{S}))$ and consider the matrices

$$\mathbf{P} = \mathbf{A}(\mathbf{S}, :) \Phi^* \Phi \mathbf{A}(:, \mathbf{S}) + \mu \mathbf{A}(\mathbf{S}, \mathbf{S}) \quad \text{and} \quad \mathbf{M} = \mathbf{A}(\mathbf{S}, :) \mathbf{A}(:, \mathbf{S}) + \mu \mathbf{A}(\mathbf{S}, \mathbf{S}).$$

By the subspace embedding property (5.5),

$$\begin{aligned}\lambda_{\max}\left(\mathbf{P}^{-1/2}\mathbf{M}\mathbf{P}^{-1/2}\right) &= \max_{\mathbf{z}\neq\mathbf{0}}\frac{\mathbf{z}^*\mathbf{M}\mathbf{z}}{\mathbf{z}^*\mathbf{P}\mathbf{z}} \leq \max_{\mathbf{z}\neq\mathbf{0}}\max\left\{1,\frac{\|\mathbf{A}(:,\mathbf{S})\mathbf{z}\|^2}{\|\Phi\mathbf{A}(:,\mathbf{S})\mathbf{z}\|^2}\right\} \leq 2; \\ \lambda_{\min}\left(\mathbf{P}^{-1/2}\mathbf{M}\mathbf{P}^{-1/2}\right) &= \min_{\mathbf{z}\neq\mathbf{0}}\frac{\mathbf{z}^*\mathbf{M}\mathbf{z}}{\mathbf{z}^*\mathbf{P}\mathbf{z}} \geq \min_{\mathbf{z}\neq\mathbf{0}}\min\left\{1,\frac{\|\mathbf{A}(:,\mathbf{S})\mathbf{z}\|^2}{\|\Phi\mathbf{A}(:,\mathbf{S})\mathbf{z}\|^2}\right\} \geq \frac{2}{3}.\end{aligned}$$

Therefore, $\kappa(\mathbf{P}^{-1/2}\mathbf{M}\mathbf{P}^{-1/2}) \leq 3$, and we apply the CG error bound (3.2) to obtain

$$\frac{\|\boldsymbol{\beta}^{(t)} - \boldsymbol{\beta}\|_{\mathbf{M}}}{\|\boldsymbol{\beta}\|_{\mathbf{M}}} \leq 2\left(\frac{\sqrt{3}-1}{\sqrt{3}+1}\right)^t \leq 2e^{-t}$$

for each $t \geq 0$, which is equivalent to the stated performance guarantee. \square

6 Conclusions

This paper has identified two leading algorithms for solving kernel ridge regression (KRR) problems with a moderate number of data points ($10^4 \leq N \leq 10^7$). The proposed algorithms based on RPCHOLESKY and KRILL preconditioning are relatively fast, robust, and reliable, outperforming previous approaches [16, 22, 23, 30, 44, 45, 53].

If the number of data points N is not prohibitively large (say, $N \leq 10^5$ – 10^6), we recommend solving the full-data KRR equations using conjugate gradient with RPCHOLESKY preconditioning. The RPCHOLESKY approach enables us solve KRR problems in just $\mathcal{O}(N^2)$ operations when the kernel matrix eigenvalues decay at a sufficiently fast polynomial rate and the chosen regularization is not too small. For example, when RPCHOLESKY preconditioning is applied to the QM9 data set with $N = 1.3 \times 10^5$ data points, 60 CG iterations are enough to achieve a high predictive accuracy.

Eigenvalue decay is the main requirement currently limiting the performance of RPCHOLESKY preconditioning, and this limitation becomes especially apparent when the regularization μ is very small (see the right panel of fig. 1). Future work is needed to discover effective preconditioners for KRR problems with slow eigenvalue decay. Existing methods based on hierarchical decompositions [3, 11, 16, 56] are a promising candidate for this purpose, but there are concerns these methods perform poorly in high dimensions [3].

If the number of data points is so large that $\mathcal{O}(N^2)$ operations is too expensive, we recommend restricting the KRR equations to $k \ll N$ data centers and solving the restricted KRR equations using conjugate gradient with KRILL preconditioning. The KRILL approach converges to the desired accuracy in just $\mathcal{O}((N+k^2)k \log k)$ operations for any kernel matrix and regularization parameter μ . For example, when KRILL preconditioning is applied to the SUSY data set with $N = 5 \times 10^6$ data points, CG converges in just 4 iterations, even with a parameter setting $\mu/N = 2 \times 10^{-10}$ that would be challenging for other algorithms.

With appropriate parameter choices and neglecting rounding errors, KRILL is guaranteed to control the condition number regardless of the regularization and the kernel matrix eigenvalue decay. Despite this success, there remain opportunities to improve on KRILL. First, the existing analysis of sparse random sign embeddings [15] does not specify appropriate values of ζ and d to use in practice. More analysis of sparse sign embeddings is needed to close the theory–practice gap; the recent paper [13] makes some progress in this direction. A second potential concern with KRILL is numerical stability; see the recent papers [21, 32]. As a practical remedy, we have addressed numerical stability by adding a small shift to the regularizer, but this approach has not been analyzed

rigorously. Finally, it may be possible to develop more efficient algorithms for restricted KRR problems when the number of data centers is $k \gg N^{1/2}$. The ideal conjugate gradient algorithm would require $\mathcal{O}(kN)$ operations, but KRILL is more expensive due to the cost of inverting the $k \times k$ preconditioner. The block Lanczos preconditioner discussed in Section 3.2 may be interesting in this setting, though—unlike KRILL—it requires spectral decay to be effective.

Acknowledgments

We would like to acknowledge helpful conversations with Misha Belkin, Tyler Chen, Riley Murray, Madeleine Udell, and Jorge Garza-Vargas.

A Data sets

In our numerical experiments, we use data from LIBSVM [10], OpenML [52], and UCI [20]. We also use the QM9 dataset [41, 43] which can be found online at <https://doi.org/10.6084/m9.figshare.c.978904.v5>. See the Github repository <https://github.com/eeeperly/Fast-Efficient-KRR-Preconditioning> for a script to download the data sets.

Table 1: Data sets used in our experiments.

Data set	Dimension d	Sample size N	Source
Testbed			
ACSIncome	11	1 331 600	OpenML
Airlines_DepDelay_1M	9	800 000	OpenML
cod_rna	8	59 535	LIBSVM
COMET_MC_SAMPLE	4	71 712	LIBSVM
connect_4	126	54 045	LIBSVM
covtype_binary	54	464 809	LIBSVM
creditcard	29	227 845	OpenML
diamonds	9	43 152	OpenML
HIGGS	28	500 000	LIBSVM
hls4ml_lhc_jets_hlf	16	664 000	OpenML
ijcnn1	22	49 990	LIBSVM
jannis	54	46 064	OpenML
Medical_Appointment	18	48 971	OpenML
MNIST	784	60 000	OpenML
sensit_vehicle	100	78 823	LIBSVM
sensorless	48	58 509	LIBSVM
volkert	180	46 648	OpenML
w8a	300	49 749	LIBSVM
YearPredictionMSD	90	463 715	LIBSVM
yolanda	100	320 000	OpenML
Additional data sets			
QM9	435	133 728	[41, 43]
SUSY	18	5 000 000	UCI

References

- [1] A. Alaoui and M. W. Mahoney. Fast randomized kernel ridge regression with statistical guarantees. In *Proceedings of the 28th International Conference on Neural Information Processing Systems*, 2015. URL <https://dl.acm.org/doi/10.5555/2969239.2969326>. 6, 13, 15
- [2] J. M. Altschuler and P. A. Parrilo. Kernel approximation on algebraic varieties. *SIAM Journal on Applied Algebra and Geometry*, 7(1):1–28, 2023. doi:10.1137/21M1425050. 7
- [3] S. Ambikasaran, D. Foreman-Mackey, L. Greengard, D. W. Hogg, and M. O’Neil. Fast direct methods for Gaussian processes. *IEEE Transactions on Pattern Analysis and Machine Intelligence*, 38(2):252–265, 2016. doi:10.1109/TPAMI.2015.2448083. 15, 23
- [4] H. Avron, P. Maymounkov, and S. Toledo. Blendenpik: Supercharging LAPACK’s least-squares solver. *SIAM Journal on Scientific Computing*, 32(3):1217–1236, 2010. doi:10.1137/090767911. 17
- [5] H. Avron, K. L. Clarkson, and D. P. Woodruff. Faster kernel ridge regression using sketching

- and preconditioning. *SIAM Journal on Matrix Analysis and Applications*, 38(4):1116–1138, 2017. doi:[10.1137/16M1105396](https://doi.org/10.1137/16M1105396). 2, 5, 6, 13, 15
- [6] F. Bach. Sharp analysis of low-rank kernel matrix approximations. In *Proceedings of the 26th Annual Conference on Learning Theory*, volume 30 of *Proceedings of Machine Learning Research*, pages 185–209, 2013. URL <https://proceedings.mlr.press/v30/Bach13.html>. 13
- [7] P. Baldi, P. Sadowski, and D. Whiteson. Searching for exotic particles in high-energy physics with deep learning. *Nature Communications*, 5(1):1–9, 2014. doi:[10.1038/ncomms5308](https://doi.org/10.1038/ncomms5308). 20
- [8] S. Blücher, K.-R. Müller, and S. Chmiela. Reconstructing kernel-based machine learning force fields with super-linear convergence. *arXiv:2212.12737*, 2022. URL <https://arxiv.org/abs/2212.12737>. 2
- [9] A. Caponnetto and E. De Vito. Optimal rates for the regularized least-squares algorithm. *Foundations of Computational Mathematics*, 7(3):331–368, 2006. doi:[10.1007/s10208-006-0196-8](https://doi.org/10.1007/s10208-006-0196-8). 4
- [10] C.-C. Chang and C.-J. Lin. LIBSVM: A library for support vector machines. *ACM Transactions on Intelligent Systems and Technology*, 2(3), 2011. doi:[10.1145/1961189.1961199](https://doi.org/10.1145/1961189.1961199). 24
- [11] J. Chen, H. Avron, and V. Sindhwani. Hierarchically compositional kernels for scalable nonparametric learning. *Journal of Machine Learning Research*, 18(66):1–42, 2017. URL <http://jmlr.org/papers/v18/15-376.html>. 15, 23
- [12] Y. Chen, E. N. Epperly, J. A. Tropp, and R. J. Webber. Randomly pivoted Cholesky: Practical approximation of a kernel matrix with few entry evaluations. *arXiv:2207.06503*, 2023. URL <https://arxiv.org/abs/2207.06503>. 2, 4, 14, 15, 22
- [13] S. Chenakkod, M. Dereziński, X. Dong, and M. Rudelson. Optimal embedding dimension for sparse subspace embeddings. In *Proceedings of the 56th Annual ACM Symposium on Theory of Computing*, 2024. doi:[10.1145/3618260.3649762](https://doi.org/10.1145/3618260.3649762). 23
- [14] K. L. Clarkson and D. P. Woodruff. Low-rank approximation and regression in input sparsity time. *Journal of the ACM*, 63(6), 2017. doi:[10.1145/3019134](https://doi.org/10.1145/3019134). 17
- [15] M. B. Cohen. Nearly tight oblivious subspace embeddings by trace inequalities. In *Proceedings of the Twenty-Seventh Annual ACM-SIAM Symposium on Discrete Algorithms*, 2016. doi:[10.1137/1.9781611974331.ch21](https://doi.org/10.1137/1.9781611974331.ch21). 2, 3, 17, 22, 23
- [16] K. Cutajar, M. Osborne, J. Cunningham, and M. Filippone. Preconditioning kernel matrices. In *Proceedings of The 33rd International Conference on Machine Learning*, 2016. URL <https://proceedings.mlr.press/v48/cutajar16.html>. 2, 6, 13, 14, 15, 23
- [17] B. Dai, B. Xie, N. He, Y. Liang, A. Raj, M.-F. F. Balcan, and L. Song. Scalable kernel methods via doubly stochastic gradients. In *Proceedings of the 27th International Conference on Neural Information Processing Systems*, 2014. URL <https://dl.acm.org/doi/10.5555/2969033.2969166>. 13
- [18] V. L. Deringer, A. P. Bartók, N. Bernstein, D. M. Wilkins, M. Ceriotti, and G. Csányi. Gaussian process regression for materials and molecules. *Chemical Reviews*, 121(16):10073–10141, 2021. doi:[10.1021/acs.chemrev.1c00022](https://doi.org/10.1021/acs.chemrev.1c00022). 1, 17

- [19] Y. Dong and P.-G. Martinsson. Simpler is better: A comparative study of randomized pivoting algorithms for CUR and interpolative decompositions. *Advances in Computational Mathematics*, 49(4):66, Aug. 2023. doi:[10.1007/s10444-023-10061-z](https://doi.org/10.1007/s10444-023-10061-z). 17
- [20] D. Dua and C. Graff. UCI machine learning repository, 2017. URL <http://archive.ics.uci.edu/ml>. 24
- [21] E. N. Epperly, M. Meier, and Y. Nakatsukasa. Fast randomized least-squares solvers can be just as accurate and stable as classical direct solvers. *arXiv:2406.03468*, 2024. URL <https://arxiv.org/abs/2406.03468>. 23
- [22] Z. Frangella, J. A. Tropp, and M. Udell. Randomized Nyström preconditioning. *SIAM Journal on Matrix Analysis and Applications*, 44(2):718–752, June 2023. ISSN 0895-4798. doi:[10.1137/21M1466244](https://doi.org/10.1137/21M1466244). 2, 5, 6, 13, 14, 15, 23
- [23] J. Gardner, G. Pleiss, K. Q. Weinberger, D. Bindel, and A. G. Wilson. GPyTorch: Blackbox matrix-matrix Gaussian process inference with GPU acceleration. In *Proceedings of the 32nd International Conference on Neural Information Processing Systems*, 2018. URL <https://dl.acm.org/doi/10.5555/3327757.3327857>. 2, 5, 13, 14, 23
- [24] G. H. Golub and C. F. Van Loan. *Matrix Computations*. Johns Hopkins University Press, 2013. doi:[10.56021/9781421407944](https://doi.org/10.56021/9781421407944). 5, 13
- [25] A. Gonen, F. Orabona, and S. Shalev-Shwartz. Solving ridge regression using sketched preconditioned SVRG. In *Proceedings of the 33rd International Conference on International Conference on Machine Learning*, 2016. URL <https://dl.acm.org/doi/10.5555/3045390.3045538>. 16
- [26] J. Lacotte and M. Pilanci. Fast convex quadratic optimization solvers with adaptive sketching-based preconditioners. *arXiv:2104.14101*, 2021. URL <https://arxiv.org/abs/2104.14101>. 17
- [27] M. Letizia, G. Losapio, M. Rando, G. Grosso, A. Wulzer, M. Pierini, M. Zanetti, and L. Rosasco. Learning new physics efficiently with nonparametric methods. *The European Physical Journal C*, 82(10):879, 2022. doi:[10.1140/epjc/s10052-022-10830-y](https://doi.org/10.1140/epjc/s10052-022-10830-y). 20
- [28] S. Ma and M. Belkin. Diving into the shallows: A computational perspective on large-scale shallow learning. In *Proceedings of the 31st International Conference on Neural Information Processing Systems*, 2017. URL <https://dl.acm.org/doi/10.5555/3294996.3295135>. 13
- [29] P.-G. Martinsson and J. A. Tropp. Randomized numerical linear algebra: Foundations and algorithms. *Acta Numerica*, 29:403–572, 2020. doi:[10.1017/S0962492920000021](https://doi.org/10.1017/S0962492920000021). 9, 13, 17
- [30] G. Meanti, L. Carratino, L. Rosasco, and A. Rudi. Kernel methods through the roof: Handling billions of points efficiently. In *Proceedings of the 34th International Conference on Neural Information Processing Systems*, 2020. URL <https://dl.acm.org/doi/abs/10.5555/3495724.3496932>. 11, 16, 23
- [31] M. Meier and Y. Nakatsukasa. Randomized algorithms for Tikhonov regularization in linear least squares. *arXiv:2203.07329*, 2022. URL <https://arxiv.org/abs/2203.07329>. 17

- [32] M. Meier, Y. Nakatsukasa, A. Townsend, and M. Webb. Are sketch-and-precondition least squares solvers numerically stable? *SIAM Journal on Matrix Analysis and Applications*, 45(2): 905–929, 2024. doi:[10.1137/23M1551973](https://doi.org/10.1137/23M1551973). 23
- [33] X. Meng, M. A. Saunders, and M. W. Mahoney. LSRN: A parallel iterative solver for strongly over- or underdetermined systems. *SIAM Journal on Scientific Computing*, 36(2):C95–C118, 2014. doi:[10.1137/120866580](https://doi.org/10.1137/120866580). 17
- [34] R. Murray, J. Demmel, M. W. Mahoney, N. B. Erichson, et al. Randomized numerical linear algebra: A perspective on the field with an eye to software. Technical report, University of California Berkeley Electrical Engineering and Computer Science, 2022. URL <https://arxiv.org/abs/2302.11474>. No. UCB/EECS-2023-19. 17
- [35] C. Musco and C. Musco. Randomized block Krylov methods for stronger and faster approximate singular value decomposition. In *Proceedings of the 28th International Conference on Neural Information Processing Systems*, 2015. URL <https://dl.acm.org/doi/10.5555/2969239.2969395>. 16
- [36] C. Musco and C. Musco. Recursive sampling for the Nyström method. In *Proceedings of the 31st International Conference on Neural Information Processing Systems*, volume 30, 2017. URL <https://dl.acm.org/doi/10.5555/3294996.3295140>. 6, 15
- [37] I. K. Ozaslan, M. Pilanci, and O. Arikan. Iterative Hessian sketch with momentum. In *IEEE International Conference on Acoustics, Speech and Signal Processing*, 2019. doi:[10.1109/ICASSP.2019.8682720](https://doi.org/10.1109/ICASSP.2019.8682720). 12
- [38] J. Parkinson and W. Wang. Linear-scaling kernels for protein sequences and small molecules outperform deep learning while providing uncertainty quantitation and improved interpretability. *Journal of Chemical Information and Modeling*, 63(15):4589–4601, 2023. doi:[10.1021/acs.jcim.3c00601](https://doi.org/10.1021/acs.jcim.3c00601). 16
- [39] M. Pilanci and M. J. Wainwright. Newton sketch: A near linear-time optimization algorithm with linear-quadratic convergence. *SIAM Journal on Optimization*, 27(1):205–245, 2017. doi:[10.1137/15M1021106](https://doi.org/10.1137/15M1021106). 17
- [40] A. Radovic, M. Williams, D. Rousseau, M. Kagan, D. Bonacorsi, A. Himmel, A. Aurisano, K. Terao, and T. Wongjirad. Machine learning at the energy and intensity frontiers of particle physics. *Nature*, 560(7716):41–48, 2018. doi:[10.1038/s41586-018-0361-2](https://doi.org/10.1038/s41586-018-0361-2). 20
- [41] R. Ramakrishnan, P. O. Dral, M. Rupp, and O. A. von Lilienfeld. Quantum chemistry structures and properties of 134 kilo molecules. *Scientific Data*, 1(1):140022, 2014. ISSN 2052-4463. doi:[10.1038/sdata.2014.22](https://doi.org/10.1038/sdata.2014.22). 17, 24, 25
- [42] V. Rokhlin and M. Tygert. A fast randomized algorithm for overdetermined linear least-squares regression. *Proceedings of the National Academy of Sciences*, 105(36):13212–13217, 2008. doi:[10.1073/pnas.0804869105](https://doi.org/10.1073/pnas.0804869105). 17
- [43] L. Ruddigkeit, R. van Deursen, L. C. Blum, and J.-L. Reymond. Enumeration of 166 billion organic small molecules in the chemical universe database GDB-17. *Journal of Chemical Information and Modeling*, 52(11):2864–2875, 2012. doi:[10.1021/ci300415d](https://doi.org/10.1021/ci300415d). 17, 24, 25

- [44] A. Rudi, L. Carratino, and L. Rosasco. FALKON: An optimal large scale kernel method. In *Proceedings of the 31st International Conference on Neural Information Processing Systems*, 2017. URL <https://dl.acm.org/doi/10.5555/3294996.3295145>. 2, 11, 16, 20, 23
- [45] A. Rudi, D. Calandriello, L. Carratino, and L. Rosasco. On fast leverage score sampling and optimal learning. In *Proceedings of the 32nd International Conference on Neural Information Processing Systems*, volume 31, 2018. URL <https://dl.acm.org/doi/10.5555/3327345.3327470>. 2, 6, 11, 15, 16, 20, 23
- [46] Y. Saad. *Iterative Methods for Sparse Linear Systems*. Society for Industrial and Applied Mathematics, second edition, 2003. doi:10.1137/1.9780898718003. 12
- [47] G. Shabat, E. Choshen, D. B. Or, and N. Carmel. Fast and accurate Gaussian kernel ridge regression using matrix decompositions for preconditioning. *SIAM Journal on Matrix Analysis and Applications*, 42(3):1073–1095, 2021. doi:10.1137/20M1343993. 2
- [48] A. Smola and P. Bartlett. Sparse greedy Gaussian process regression. In *Proceedings of the 13th International Conference on Neural Information Processing Systems*, volume 13, 2000. URL <https://dl.acm.org/doi/10.5555/3008751.3008838>. 2, 8
- [49] A. Stuke, M. Todorović, M. Rupp, C. Kunkel, K. Ghosh, L. Himanen, and P. Rinke. Chemical diversity in molecular orbital energy predictions with kernel ridge regression. *The Journal of Chemical Physics*, 150(20):204121, 2019. doi:10.1063/1.5086105. 17, 18
- [50] J. A. Tropp, A. Yurtsever, M. Udell, and V. Cevher. Streaming low-rank matrix approximation with an application to scientific simulation. *SIAM Journal on Scientific Computing*, 41(4):A2430–A2463, 2019. doi:10.1137/18M1201068. 9
- [51] O. T. Unke, S. Chmiela, H. E. Sauceda, M. Gastegger, I. Poltavsky, K. T. Schütt, A. Tkatchenko, and K.-R. Müller. Machine learning force fields. *Chemical Reviews*, 121(16):10142–10186, 2021. doi:10.1021/acs.chemrev.0c01111. 2
- [52] J. Vanschoren, J. N. van Rijn, B. Bischl, and L. Torgo. OpenML: Networked science in machine learning. *ACM Special Interest Group on Knowledge Discovery in Data Explorations Newsletter*, 15(2):49–60, 2013. doi:10.1145/2641190.2641198. 24
- [53] K. Wang, G. Pleiss, J. Gardner, S. Tyree, K. Q. Weinberger, and A. G. Wilson. Exact Gaussian processes on a million data points. In *Proceedings of the 33rd International Conference on Neural Information Processing Systems*, 2019. URL <https://dl.acm.org/doi/10.5555/3454287.3455599>. 5, 13, 14, 23
- [54] J. Westermayr and P. Marquetand. Machine learning for electronically excited states of molecules. *Chemical Reviews*, 121(16):9873–9926, 2021. doi:10.1021/acs.chemrev.0c00749. 1, 17
- [55] T. Yang, Y.-f. Li, M. Mahdavi, R. Jin, and Z.-H. Zhou. Nyström method vs random Fourier features: A theoretical and empirical comparison. In *Proceedings of the 25th International Conference on Neural Information Processing Systems*, 2012. URL <https://dl.acm.org/doi/abs/10.5555/2999134.2999188>. 15
- [56] C. D. Yu, J. Levitt, S. Reiz, and G. Biros. Geometry-oblivious FMM for compressing dense SPD matrices. In *Proceedings of the International Conference for High Performance Computing, Networking, Storage and Analysis*, 2017. doi:10.1145/3126908.3126921. 15, 23